Bachelor Thesis

Degree Project in
Geological Sciences, 30 hp

North Atlantic Climate Signals in SW-Sweden: A Multi-Proxy Lake-Sediment Perspective from the Deglaciation (15.5–11 ka BP)

Sandra Zyla

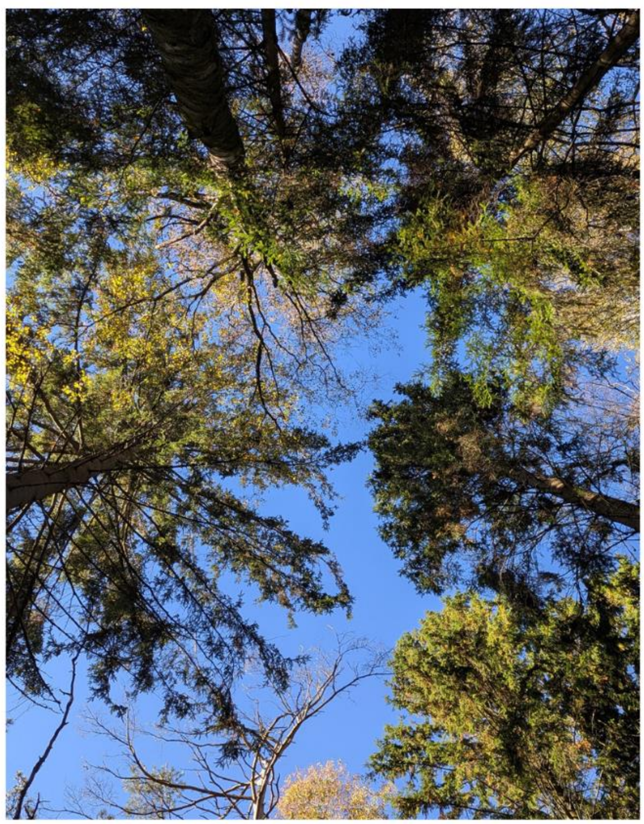

Stockholm 2026

Department of Geological Sciences
Stockholm University
SE-106 91 Stockholm

North Atlantic Climate Signals in SW-Sweden: A Multi-Proxy Lake-Sediment Perspective from the Deglaciation (15.5–11 ka BP)

Sandra Zyla

Bachelor's Degree Project in
Geological Sciences
Bachelor level 30 hp,
Course code GG6132
Spring term 2026
Supervisor: Frederik Schenk
Sarah Greenwood
Ylva Palmgren
Department of Geological Science

Abstract

The Last Deglacial period (15.5-11.0 ka BP) in Sweden was characterized by rapid environmental alteration associated with retreat of the Fennoscandian Ice Sheet. Coastline was especially affected by relative sea level fell, and input of meltwater into the global ocean. The west coast of the country was additionally impacted by oceanic changes, and Atlantic meridional overturning circulation (AMOC) shifts. This study investigates palaeoclimate and AMOC impact on southwest Sweden by using multi-proxy approach.

Here I compared published and unpublished proxy data where after adjusting dataset to common timescale, I compared trend and timing of results, in order to gain a more solid understanding of mechanisms and impacts of abrupt climate shifts. I used lake sediments from Atteköpsmosse and Käringnmossen in Halland, southwest Sweden, July Temperature reconstruction for Atteköpsmosse, $^{231}Pa/^{230}Th$ ratio from North Atlantic Ocean marine sediment core, oxygen isotope ($\delta^{18}O$) and calcium ion [Ca^{2+}] records from Greenland ice cores and form a reconstruction of highest coastline for southwest Sweden based on data package available on the Sveriges Geologiska Undersökning website.

The results indicate that climate of southwest Sweden was closely linked to oceanic changes and AMOC dynamic. The pollen proportion and temperature reconstruction for southwest Sweden follow trends observed in the high-resolution Greenland ice cores proxy, which document climatic shifts associated with weaker or stronger meridional circulation during the studied interval.

Furthermore, the study highlights the value of multi-proxy approaches in regards of palaeoclimate reconstruction based on multi-regional archives.

Table of content

1. Introduction

The Late Glacial period was characterized by dynamic climatic shifts following the Last Glacial Maximum. During 15.5-11.0 ka BP interval, significant cooling and warming events can be observed in a number of archives. The Oldest, Older and Younger Dryas were periods characterized by persistent cold and dry climate; the climate of Bølling–Allerød however, remained warm and wetter, creating a favorable condition for i.e. vegetation. The Scandinavian environment experienced abrupt and significant alteration. The impact of the Fennoscandian Ice Sheet retreat during the deglaciation led to a series of environmental changes i.e. an isostatic rebound, formation of new lakes and landforms, and the release of large amounts of meltwater into the global ocean, resulting in sea level rise (Huges *et al.*, 2016; Suzuki *et al.*, 2026). Consequently, these shaped environments and palaeoclimate along vast regions of North Atlantic including Greenland and southwest Sweden.

Proxy archives preserve indirect evidence of environmental and climatic conditions which, as a result, help understand past climate variables. Their integration from different environmental systems allows for comparison of climatic responses across local, regional, and large-scale systems. However, some of the responses can be delayed or may not provide comparable temporal resolution or climatic sensitivity in comparison to others.

Given the strong influence of prevailing climate and landscape conditions on vegetation, the studies often investigate the specific climatic tolerance regimes of individual taxa. The results can be presented by transfer functions and statistical models. The nuances in pollen proxy results can indicate somewhat individual environmental characteristics of the studied areas. This process helps to re-create past ecosystems to some extent and track the palaeoclimate variabilities. Pollen directly responds to climatic and environmental changes; hence it is among the most widely used terrestrial proxy. Located in close proximity to the southwest coastline of Sweden, sedimentary archives from Atteköpsmosse and Käringmossen, together with reconstruction of the highest coastline from approximately 13.5 ka BP, and Greenland Ice Cores provide valuable resources to investigate local palaeoclimate responses to changes in AMOC dynamics.

The single-proxy approach provides limited temporal resolution and may fail to document shorter, less pronounced events which play an important role in the reconstruction of palaeoenvironment. An assemblage of terrestrial and marine proxies expresses more comprehensive palaeoclimate reconstruction across local, regional and global climate history, and enables a cross-verification of reconstruction which can corroborate or refute an interpretation.

The anthropogenic influence on the modern climate system interferes with the integrity of the world's ice cover. The present-day climate differs from the Late Glacial period; however, the issue emerges in regard to potential consequences of abrupt climate changes, which has been an important subject of many debates in the past decades.

The relationship between ocean-atmospheric systems is and will be monitored in the years to come, to assess the real risk caused by collapse or decline of AMOC. It also remains uncertain to what extent topography and changing shorelines of SW Sweden influenced local response to AMOC-driven climate change during 15.5-11.0 ka BP.

The study of late glacial period climate variability is important because environmental changes from between 15.5 and 11.0 ka BP significantly transformed the environment across vast regions situated along the path of global ocean circulation. This offers an analogue for climate reconstruction. Therefore, understanding the previous chain of events can provide essential knowledge which allows to improve calibration of predictive models and isolate ecological tipping points. Regarding modern climate change, palaeoclimate variability serves as the integral data needed for local, regional and global risk assessment and designing an early warning system.

The main aim of this study was to integrate multiproxy palaeoclimate data covering 15.5-11.0 ka BP. Based on the results, this thesis addresses the following research questions:

- What are the main climate impacts on SW-Sweden in response to Atlantic Meridional Overturning Circulation (AMOC) disruptions?
- How did climate shift affect vegetation changes reflected by new pollen data?
- How did large-scale climate shifts originate from the North Atlantic impact local climate and vegetation in SW-Sweden?

To address the topic, records from Atteköpsmosse and Käringmossen in Halland, southwest Sweden were compared with records from the NGRIP, GRIP and GISP2 ice cores in Greenland, as well as marine records from Bermuda Rise in the North Atlantic. Assembled results evaluate synchrony of changes in Scandinavia and North Atlantic climate variability during the Late Glacial period.

2. Background

2.1. Late-glacial palaeoclimate in Scandinavia

Late deglacial period

The late deglacial period describes the interval between the Last Glacial Maximum (LGM) approximately 26,500-20,000 calibrated years Before Present (cal yr BP), and the onset of the Holocene at around 11.7 kilo annum Before Present (ka BP) (Clark *et al.*, 2009; Lowe and Walker, 2014). During the LGM, Fennoscandia was covered by several-kilometre-thick ice sheets known as the Fennoscandian Ice Sheet (FIS) (Clark *et al.*, 2009). Deglaciation of FIS began after approximately 20,000 cal yr BP and continued until the Fennoscandian region was completely ice-free by approximately 10,000-9,000 cal yr BP (Hughes *et al.*, 2016; Stroeven *et al.*, 2016). Based on the Fennoscandian deglaciation reconstruction by Hughes *et al.* (2016), Halland became fully ice-free by approximately 14,000 cal yr BP, following the onset of major regional deglaciation between 18,000 and 17,000 cal yr BP. The dynamics and timing of deglaciation is still subject to debate (Hughes *et al.*, 2016; Stroeven *et al.*, 2016).

The expansion and contraction of ice sheets on Earth results in significant pressure on the crust, leading to a glacio-isostatic change. As a result, some areas were below global sea level while the FIS depressed the crust. As the ice sheet retreated, a postglacial rebound took place and allowed the crust to gradually adjust over time to reach its equilibrium. Former shorelines adjusted during that process, can be now found across inland areas. It was a substantial factor causing relative sea-level changes throughout the Quaternary. (Lowe and Walker, 2014). In places like Gulf of Bothnia in northern Sweden, where the ice sheet retreated last, the uplift is still taking place with an approximately *c.*9 $mmyr^{-1}$ rate in Västerbotten (Ågren and Svensson, 2006).

Southern Sweden began to experience a rapid isostatic rebound at the time of FIS retreat after the LGM. The sea level rise was inadequate to the uplift, resulting in a fall of relative sea-levels along the west coast (Berglund, 1995). Atteköpsmosse and Käringmossen are located near Kattegat Strait and have since transitioned from a near-coastal to more inland position during the Holocene.

INTIMATE and 15.5-11.0 ka BP, stadials and interstadials

The general trend during last deglacial period was distinguished by gradual climate warming; however, it included occasional short-lived cooling events and abrupt climatic oscillations.
Rapid climatic shifts recorded in Greenland ice cores during the last glacial period are known as Dansgaard-Oeschger (D-O) events, named after palaeoclimatologists Willi Dansgaard and Hans Oeschger. These events alternate between cold (stadial) and relatively mild (interstadial) climatic conditions. The events were further subdivided into substadials and subinterstadials (Rasmussen *et al.*, 2014).

The shifts in atmospheric and oceanic conditions associated with these events are observed in climate-sensitive proxy records, especially isotopic oxygen ($\delta^{18}O$) ratio and calcium ion [Ca^{2+}] concentrations encapsulated in ice cores. The duration of interstadials and stadials takes between centuries and millennia. While interstadials surface air temperature decreases gradually, with relatively abrupt change to stadial conditions, the stadials are characterized as more stable and climate and more gradual in changes (Rasmussen *et al.*, 2014).

The period between 15.5 and 11.0 ka BP, was divided into an event stratigraphy proposed by Björk *et al.* (1998) as a part of the INTegrating Ice-core, MArine, and TErrestial records (INTIMATE) project. The project integrates a range of proxy records to form a stratigraphy scheme of climate events and sub-events. It initially presented the structure of North Atlantic Event Stratigraphy for the Last Termination 11.05-23.05 ka BP using Greenland Ice-Core Project (GRIP) records identified by Björk *et al.* (1998); extending back to 30.05 ka BP by using North Greenland Ice-Core Project (NGRIP) ice core records by Lowe *et al.* (2008) and subsequently to 48.05 ka BP by Blockley *et al.* (2012). The combined data from NGRIP, GRIP and Greenland Ice Sheet Project 2 (GISP2) ice cores allowed Rasmussen *et al.* (2014) to define event onsets of climate as far back as 104.05 ka BP (Rasmussen *et al.*, 2014; Lowe and Walker, 2014).

This thesis focusses on the time period between 15.5 and 11.0 ka BP, which INTIMATE event stratigraphy defines stadial episodes *Greenland Stadials 1* (GS-1) and *2* (GS-2); and interstadial episodes *Greenland Interstadial 1* (GI-1) and *2* (GI-2) (Björk *et al.*, 1998). GI-1 was further divided into seven events. The final part of GS-2.1a overlaps with the interval of study and is included in majority proxy records. Table 1, adapted from Rasmussen *et al.* (2014) includes the Greenland events and climatic periods. (Rasmussen *et al.*, 2014; Björk *et al.*, 1998).

Table 1. Table of stratigraphic events
Fragment of table from Rasmussen et al. (2014) describing onsets of events in the updated and extended INTIMATE event stratigraphy along overlapping climatic periods. A synchronized, color-coded timeline is mapped across Figures 4 and 6 to ensure temporal consistency in the analysis. Dark grey was used to mark Greenland Stadial (GS), light grey was used for Greenland Interstadials (GI) and light pink was used to distinguish alternating substadials within GI-1.

Event	**NGRIP depth (m)**	**Age (b2k) and definition uncertainty**	**Climatic periods**	**Approximate onset of climatic periods**
End of 11.4 ka BP event	1476.16	11,400	Holocene	
Start of 11.4 ka BP event	1482.32	11,520	Holocene	
Start of Holocene	1492.45	11,703 ± 4	Holocene	~11,700
Start of GS-1	1526.52	12,896 ± 4	Younger Dryas	~12,900
Start of GI-1a	1534.5	13,099	Allerød	
Start of GI-1b	1542.1	13,311	Allerød	
Start of GI-1c1	1554.75	13,600	Allerød	
Start of GI-1c2	1557.08	13,660	Allerød	
Start of GI-1c3	1570.5	13,954	Allerød	~13,900
Start of GI-1d	1574.8	14,075	Older Dryas	~14,100
Start of GI-1e	1604.64	14,692 ± 4	Bølling	~14,600
Start of GS-2.1a	1669.09	17,480	The Oldest Dryas	~18,000

Climatic periods in Scandinavia

The end of LGM marked an abrupt shift in climate. After sustained and extensive cold climate, where ice sheet dominated in Scandinavia, the gradual warming of the climate forced the ice sheets to retreat. Palaeological reconstruction from Swedish and Danish lake sediments presents distinctive two warmer periods- Bølling and Allerød. The period was occasionally interrupted by shorter climatic decline and longer cold climate following. Traditionally, we use named chronozones the Oldest Dryas, Bølling, Older Dryas, Allerød, and Younger Dryas which were originally from Denmark and assigned for main use in Scandinavian palaeoecological events. However, these become common in Quaternary literature and other geological contexts across northern Atlantic region (Rasmussen *et al.*, 2014). These chronozones are not equivalent to names for GI or GS; although, the events often overlap with the onset of climatic periods (Rasmussen *et al.*, 2014).

The Oldest Dryas- an abrupt cold period just before the onset of Bølling. Based on the INTIMATE event stratigraphy, the onset of the Oldest Dryas overlaps with GS-2.1a event which began at approximately 17.55 ka BP (Rasmussen *et al.*, 2014). In Scandinavia, it is characterized by cold however, over time a very gradual increase in temperature leading to the onset of next period (Wohlfarth *et al*., 2014).

Bølling-Allerød (or the Bølling-Allerød chronozone, BA, also DO1) mild climatic interval during Late Glacial period. This interstadial is divided into five subunits, where its onset aligns with subinterstadial GI-1e at approximately 14.6 ka BP. The warmer climate persisted until the onset of the Younger Dryas at approximately 12.9 ka BP. The BA period includes a few brief colder climates, including Older Dryas whose onset is marked at 14.1 ka BP, overlapping the GI-1d event. (Rasmussen *et al.*, 2014; Lowe and Walker, 2014). The warming climatic trend persisted during this chronozone (Wolfarth *et al*., 2014). The landscape alteration during this time was heavily influenced by the significant sea-level rise (some places approximately 25 m) caused by meltwater discharge from the ice sheet (Suzuki *et al.*, 2026) and rapid postglacial isostatic uplift followed by continuous retreat of the ice sheet (Berglund *et al.*, 1994).

Younger Dryas (also Younger Dryas chronozone, YD) the stadial from approximately 12.95-11.75 ka BP and overlaping GS-1 event (Table 1.) (Rasmussen *et al*., 2014). This cold period significantly slowed down or locally halted the retreat of ice sheets across Scandinavia and the North Atlantic regions. The changes in the environment can be observed in many proxy records (Ruddiman, 2013). After the general warming trend of BA, YD is characterized by a colder and arid climate. The abrupt climate warming of Holocene brought an end to the cold Younger Dryas period (Lowe and Walker, 2014).

Holocene- the most recent geological epoch, which starts at approximately 11.75 ka BP and continues until present day (Rasmussen *et al.*, 2014; Lowe and Walker, 2014). It is characterized by a warm and stable climatic trend, but what distinguishes this period from the others is the integral involvement and evolution of human environments (Lowe and Walker, 2014). This relatively stable climatic period shows less frequent and shorter fluctuation in environmental change based on Greenland oxygen isotope records (Lowe and Walker, 2014; Rasmussen *et al.*, 2014).

2.2. Biological proxies of past climate variability

Traditionally, climate reconstruction has been based on biological proxies, which reflect climate tolerance of different taxa and assemblages. This thesis uses chironomid and pollen archives from southwest Sweden in order to reconstruct climatic conditions and environmental variability during the interval 15.5-11.0 ka BP.

2.2.1. Chironomidae

Chironomidae are non-biting midges, members of the Diptera order (true flies). Their abundance and composition in freshwater habitats depend on factors such as pH, salinity, depth of water, temperature, oxygen concentration, and trophic status. The head capsule of the larval stage is the most preserved remains in the sediments, which can be identified and have been extensively analyzed to estimate palaeotemperature. Distribution of Chironomidae species is closely related to the summer air and surface water temperature (Lowe and Walker, 2014).

2.2.2. Pollen

Pollen analysis is one of the widely used methods employed in the reconstruction of palaeoenvironments. Palynology was first developed in the 1920s, allowing for correlation of local and even continental-marine stratigraphic units. Abundantly produced pollen grains and spores remain on the ground, while some of them accumulate in water bodies, subsequently becoming integrated and fossilized in sediments. Pollen analysis requires the extraction, identification, and quantification of these remains, preferably from lacustrine or peat deposits (Lowe and Walker, 2014). Since different plants are adapted to different growing conditions, it is possible to reconstruct past climates and environments by looking at abundance and taxonomic composition of fossil pollen in sedimentary archives.

2.2.2a. *Betula*

Betula, commonly known as a birch, can be found occurring naturally across most of Europe, extending eastwards into central Siberia. These broadleaved, deciduous trees often thrive on relatively fertile, light and well-drained soil under somewhat acidic conditions and do not tolerate shade or prolonged summer drought (Beck *et al*., 2016).
Birch trees are monoecious meaning, both female and male reproductive organs occur on one the same individual and produce abundant wind-pollinated seeds and pollen, which can be dispersed over long distances. These begin to flower at 20-25 years of age, but free-standing individuals may flower already at 10 years old of age. *Betula* grows to approximately 20 m tall and lives up to 100 years (Beck *et al.*, 2016).

2.2.2b. Pinus

Pinus commonly pine, occur in a wide range of sizes. The genus comprises 95 species and forms hybrids along the vast dispersal region (Krugman and Jenkinson, 1974). Pinus sylvestris (Scotch pine) has a broad distribution ranging from Spain to the far east Russia. It is also the only native pine species in Scandinavia. Pine grows at a wide range of elevation- from sea level to over 2600m in the Caucasus. As a pioneer species, it can grow on very poor-nutrient soils and is frost and drought tolerant with imbedded stomata and a waxy layer on the epidermis to protect the needle from water loss (Houstan Durrant et al., 2016).

These evergreen trees are monoecious, where male cones are located on lower branches and female on the tips of new, and strong shoots. The cones open after alternating periods of wet and dry weather, allowing winged seeds to be distributed by wind. The Scotch pine is light-liking species, and some of the pine representants can live on average for 400 years and grow up to 27m (Houstan Durrant *et al.,* 2016).

2.2.2c. *Artemisia*

The genus *Artemisa* comprises over 400 species and is predominantly distributed across the Northern Hemisphere. These are mostly perennial herbs and shrubs, commonly found in Asia, Europe and North America, however these occur on every continent except Antarctica (Wright, 2002). In the palaeoecological literature, *Artemisia* pollen is often referred without further taxonomy due to its morphological homogeneity under light microscopy across the large number of species (Rull, 2025). The genus has a wide range of tall shrubs to dwarf herbaceous alpine form, and can be slow-growing, cold-enduring, hard-wooded shrubs (Wright, 2002). *Artemisia* pollen can be used as an essential component and useful bioindicator for identifying open landscapes and sometimes proxy for aridity and dry climate (Lu *et al.*, 2022).

2.2.2d. *Oxyria /Rumex acetosella*

Oxyria digyna and *Rumex acetosella L.* are perennial herbaceous species members of the Polygonaceae family. Different literature and different identification keys use different pollen-type nomenclature for small *Rumex*-like pollen grains, some calling them *Oxyria*-type, others *Rumex acetosella L*. Their pollen exhibit morphological similarities and can be difficult to distinguish. In this study, they are therefore assumed to be the same *Oxyria*-type pollen, despite being distict species within the Polygonaceae family (Ylva Palmgren, personal communication 2026-05-26). *Oxyria* are found across arctic-alpine circumpolar environments, as well as in the mountains of Europe, Asia, and North America (Mooney and Billings, 1961). This pioneer species is well adapted to challenging environmental conditions, including cold temperatures, high altitudes, nutrient-poor and underdeveloped soils (Li *et al.*, 2024). *Rumex acetossella L.* mature seeds-nuts are wind pollinated or dispersed by other animals, such as ants. Seed size can depend on the environment in which they grow. The herb is dioecious, with male and female reproductive organs on separate individual plant (Houssard and Escarre, 1991).

2.2.2e. *Poaceae/ Gramineae*

Poaceae, commonly grasses, are widespread and diverse plant families, occurring in most biogeographical zones. With over 10,000 species and several subfamilies, these rank among the most abundant in terms of biodiversity globally (Van Haeften *et al.*, 2024). Members of *Poaceae* adapt to a range of climate regimes and soils, including arid and aquatic environment. Due to their abundance and widespread distribution, *Poaceae* contributes to reconstruction of palaeoecological studies with a focus on vegetation, environmental conditions, and climate change (Wei *et al.*, 2023).

2.2.2f. *Ericaceae*

Ericaceae is a diverse family of evergreen, sometimes deciduous shrubs reaching over 4,100 species. Members of this family can easily adapt to different environmental and geographical conditions growing in habitats with acidic, nutrient-poor soils and rich in organic matter, such as heaths or peat bogs. These adapt in the Arctic and temperate regions of Eurasia, to Central and South America, and Mediterranean climates. The family is heliophilous (light-demanding) and pollen from woody *Ericaceae* shows uniform pollen morphology and 23-82 µm in diameter (Stevens *et al.*, 2004; Kubitzki and Kadereit, 2004).

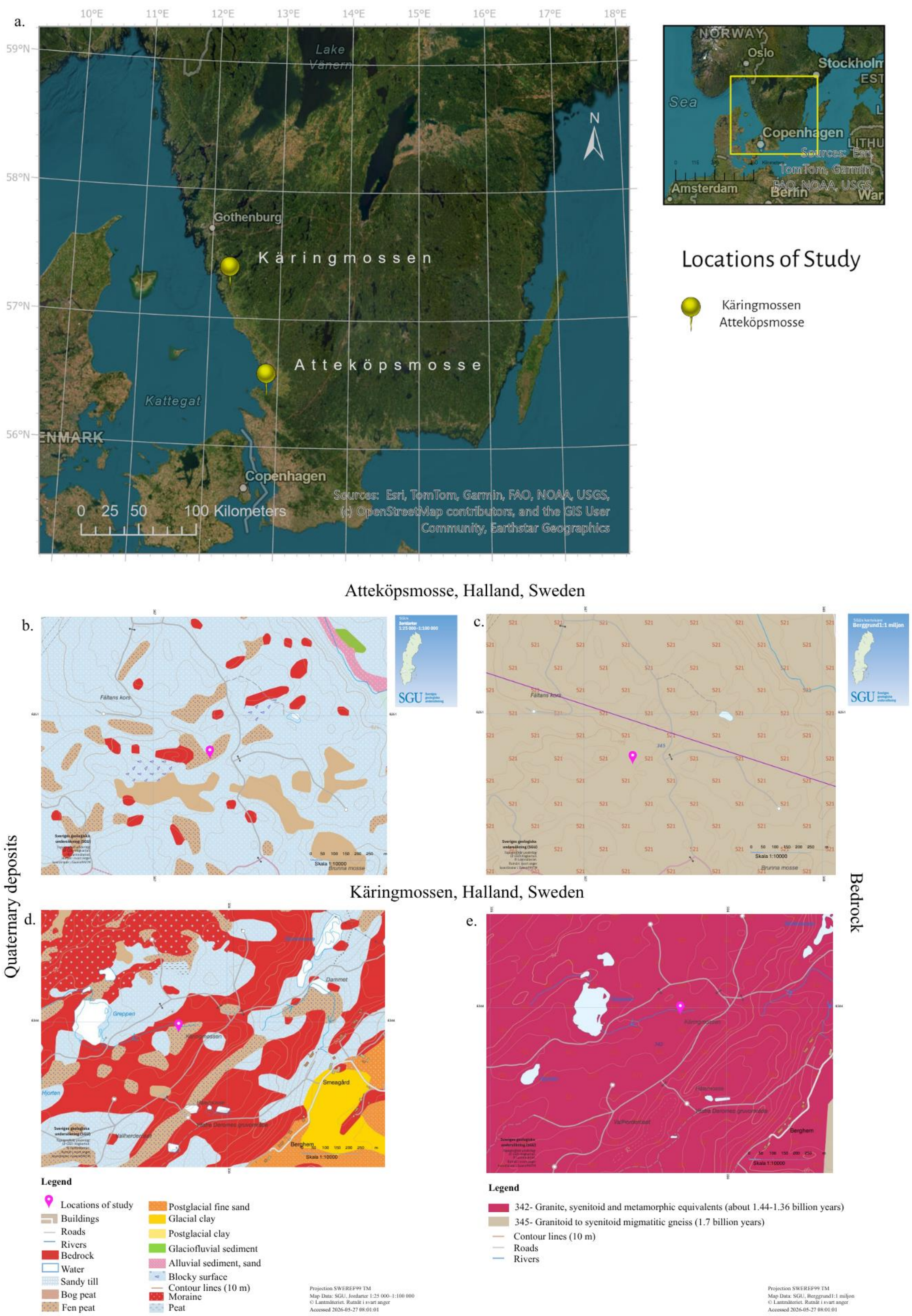
a.
Lake Vänern
Gothenburg
Käringmossen
Atteköpsmosse
Kattegat
Copenhagen
0 25 50 100 Kilometers
Sources: Esri, TomTom, Garmin, FAO, NOAA, USGS, (c) OpenStreetMap contributors, and the GIS User Community, Earthstar Geographics
Locations of Study
Käringmossen
Atteköpsmosse
Atteköpsmosse, Halland, Sweden
b.
c.
Käringmossen, Halland, Sweden
d.
e.
Quaternary deposits
Bedrock
Legend
Locations of study
Buildings
Roads
Rivers
Bedrock
Water
Sandy till
Bog peat
Fen peat
Postglacial fine sand
Glacial clay
Postglacial clay
Glaciofluvial sediment
Alluvial sediment, sand
Blocky surface
Contour lines (10 m)
Moraine
Peat
Legend
342- Granite, syenitoid and metamorphic equivalents (about 1.44-1.36 billion years)
345- Granitoid to syenitoid migmatitic gneiss (1.7 billion years)
Contour lines (10 m)
Roads
Rivers

Figure 1. Location, quaternary deposits, and bedrock geology of the study sites in southwest Sweden.
a. location of the peatland study sites Käringmossen (57°12′34.2″N, 12°16′52.7″E) and Atteköpsmosse (56°23′00″N, 12°51′00″E) in Halland County, southwest Sweden; b. Quaternary deposits surrounding Atteköpsmosse; c. bedrock geology of Atteköpsmosse; d. Quaternary deposits surrounding Käringmossen; e. bedrock geology of Käringmossen.

Basemap for panel (a): ArcGIS Pro; coordinate system: SWEREF 99 TM. Geological and quaternary deposit data for panels (b–e) obtained from the Geological Survey of Sweden (SGU; www.sgu.se).

2.3. Palaeoclimate records used in this study

2.3.1. Atteköpsmosse, Halland, Sweden

Located in Halland, Atteköpsmosse (56°23'N, 12°51'E) (Fig. 1a) is currently a small wetland and has been the focus of numerous studies by Wohlfarth *et al.* (2018). The site is currently situated at 188 m a.s.l.(Google Earth Pro, 2025) on the northwest-southeast trending horst Hallandsåsen (Wohlfarth *et al.*, 2018). The nearest identified highest coastline record for Bjäre Peninsula is 65 meters above sea level (m a.s.l.) which dated to 13,900 years BP (Påsse and Daniels, 2015). Thus, the site remained above sea level during deglaciation (Wohlfarth *et al.*, 2018). Based on Sveriges Geologiska Undersökning-Swedish Geological Survey (SGU), the local bedrock is granite and syenitoid, which were formed approximately 1.7 Ga years ago (Fig. 1c) during the Svekonorwegian Orogen and is covered by Quaternary deposits including sandy till, blocky surface on sandy till, alluvial sediment-sand and glaciofluvial sediment, and occasional peatlands (Fig. 1b) (SGU, no date).

The site was sampled in 1981, 2000, and 2011 producing cores C-1981, C-2000 and C-2011, respectively, using a Russian peat corer (7.5 cm and 5 cm diameter and 1 m long) (Wohlfarth *et al.*, 2018). Core C-1981 reached a depth of 600 cm. Wohlfarth et al. (2018) used C-1981 core to describe pollen distribution at 32 different depths and lithostratigraphic analysis. The latter were identified as follow: 600-575 cm partly organic silts and sands, 575-542 cm gyttja silt, 542-482 cm silty gyttja, 483-444 cm fine detritus gyttja, 444-427 cm silty gyttja and 427-380 cm coarse detritus gyttja. The lowermost lithological units suggest high runoff and sedimentation rates with infilling of the basin at the uppermost sediments based on a rise in organic matter (Wohlfarth *et al.*, 2018).

Because the C-1981 core was missing its own radiocarbon chronology, Wohlfarth *et al.* (2018) established a core-to-core stratigraphic alignment using the C-2011 chronology as the reference sequence, thereby enabling an optimal correlation between the two records. The authors constructed age-depth model for the C-2011 core using 37 AMS ^{14}C dates calibrated with IntCal13 calibration curve. The process relied on stratigraphical alignment based on Loss of Ignition (LOI) records data from both cores, with C-2011 being reference sequence; the Monte Carlo approach was used to perform stratigraphic alignments, providing a comprehensive set of possible alignments between records (Wohlfarth *et al.*, 2018).

2.3.2 Käringmossen, Halland, Sweden

Data used in this study was gathered by Palmgren (2023) from Käringmossen (57°12'34.2"N, 12°16'52.7"E), Halland in southwestern Sweden (Fig. 1a). The nearest highest coastline record was identified in Varberg at approximately 73 m a.s.l on the west side and 77 m a.s.l. on the east side of the city and dated to approximately 13,500 and 13,450 yr BP respectively (Påsse, 1990; Påsse and Daniels, 2015). Käringmossen is currently situated at approximately 80 m a.s.l., suggesting that it was about 3-7 m above the highest coastline (Palmgren, 2023). The area is about 5 km east away from the Swedish west coast (Nordqvist, 2003). According to SGU, the local bedrock consists of granite, syenitoid and metamorphic equivalents from Sveconorwegian Orogen and is dated to approximately 1.44-1.36 Ga (Fig. 1e); it is also covered by thin Quaternary deposits i.e. sandy till, glacial and postglacial clay, postglacial fine sand and peatlands (Fig. 1d) (SGU, no date).

Fieldwork took place in June 14th and 15th 2022 in Käringmossen peatland, after initial unsuccessful attempt of retrieving core deeper than 2 m from Skatmossen peatland. A Russian peat corer (length of 1 m, diameter 4 cm) was used to extract the master core, KÄR01, which reached a depth of 469cm. The master core was assembled from five 1 m sections. In addition, nine supporting cores were retrieved covering 0-471 cm depths, providing record of the transition from lacustrine to wetland environments throughout the stratigraphic section (Palmgren, 2023).

The sediments sequences were identified by Palmgren (2023) as follows: from 469-389 cm clay gyttja with medium to coarse sand, 389- 352 cm clay gyttja, 352-293 cm gyttja, 293-273 cm fen peat, 273-245 cm *sphagnum* peat, 245-165 cm fen peat, 165-0 cm *sphagnum* peat.

A chronology of the retrieved section was based on 13 radiocarbon dates and 1 identified tephra: Vedde ash (age ca 12.1 ka BP). Radiocarbon dating used accelerator mass spectrometry (AMS), and produced a calibrated age-date model which showed a median age of –72 at the shallowest 0 cm depth and 15,202 cal yr BP at the deepest sampled depth from 469 cm (Palmgren, 2023).

2.3.3. Greenland ice core records

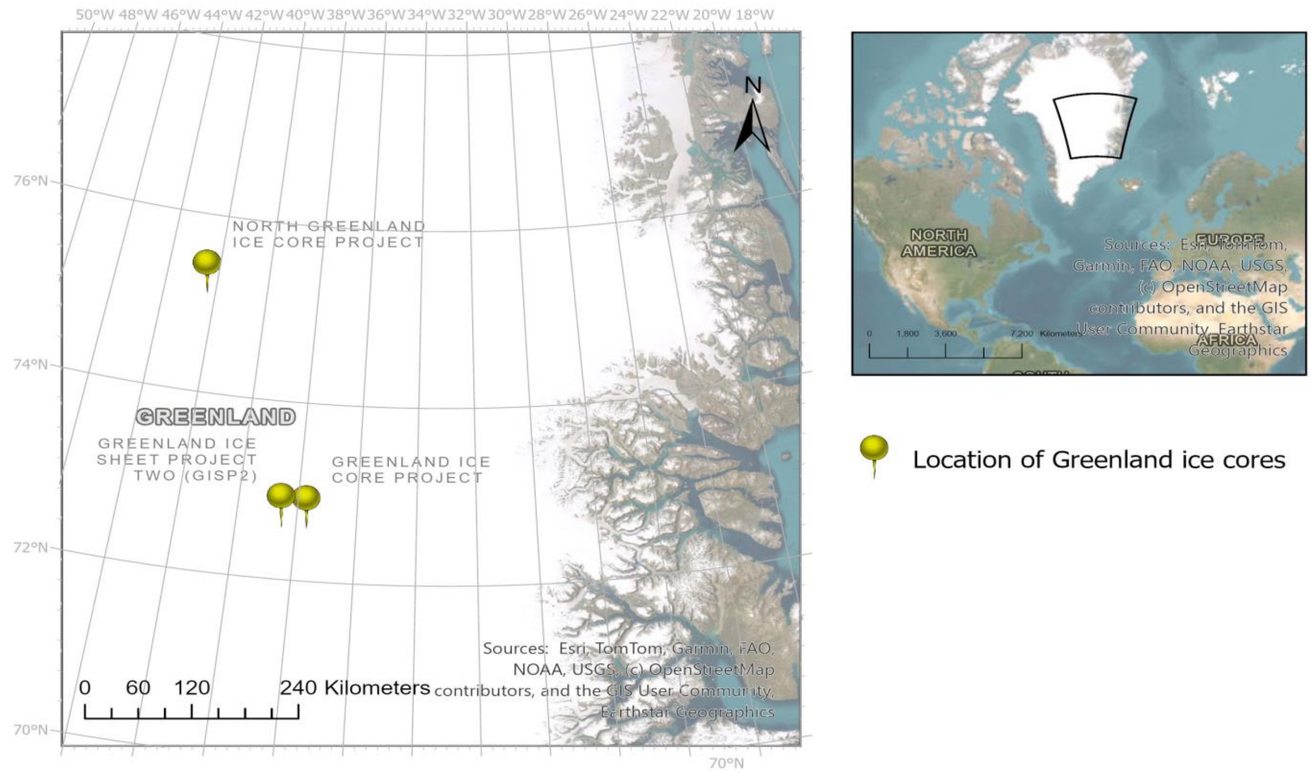

Figure 2. Map of Greenland Ice Core projects.
Location of GRIP (72.57°N, 37.62°W), NGRIP (75.10°N, 42.32°W) and GISP2 (72.35°N, 38.28°W)in Greenland.

Basemap: ArcGIS Pro; Coordinate System: WGS 84 / Arctic Polar Stereographic

The Greenland Ice-Core Project (GRIP) is located at 72.57°N, 37.62°W (Fig. 2). was drilled between 1986-1992, reaching 3028.8 m in length. The site was located at 3232 m a.s.l. with the present-day accumulation of 0.23 m ice yr^{-1} (Rasmussen *et al.,* 2023).

The Greenland Ice Sheet Project 2 (GISP2) was a five-year project completed in 1993, recovering a 3,053.44 m long ice core. GISP2 covers 100 000 years of detailed oxygen isotope profile. Situated at 72.35°N, 38.28°W (Fig. 2).

The North Greenland Ice-Core Project (NGRIP) began drilling in 1996 and was completed in 2003. The drilling site was located at 75.10° N, 42.32°W in central Greenland at an elevation of 2917 m above sea level (Fig. 2). The annual layers are more than 5 mm thick through NGRIP ice core allowing high-resolution of climate reconstruction. Due to technical difficulties at 1372 m depth, this Greenland record is combined of two ice cores, NGRIP1 and NGRIP2. The operation proceeded, and the latter continued from 1346 m (corresponding to approximately 9.55 ka BP) overlapping with NGRIP1 to ensure correct alignment of the records, hence NGRIP2 will be used in this thesis (Rasmussen *et al.*, 2023; Andersen *et al.*, 2004).

NGRIP ice- core served as a base for development of the event stratigraphy using the annual-layer of high-resolution timeline called Greenland Ice Core Chronology 2005 (GICC05) (Rasmussen *et al.*,2014) as well as INTIMATE project (Rasmussen *et al.*, 2014). GRIP, GISP2 and NGRIP were synchronized and put on a common timescale. The ages are expressed in years before AD 2000 (b2k), with radiocarbon ages reported in years BP where present is defined as 1950 CE. The GICC05 ages are 50 years offset to radiocarbon ages (Lowe and Walker, 2014). The chronology extends to 60 ka, first stated in Lowe *et al.* 200, where the 15.5-11.0 ka BP interval is constructed by combining data from GRIP and both parts of NGRIP cores (Rasmussen *et al*., 2014; Lowe and Walker, 2014). Development of GICC21 has been introduced by Sinnl *et al.* (2022) and the underlaying data is available Rasmussen *et al.* (2023).

Changes in $\delta^{18}O$ values in the ice-sheet layers serve as a primary proxy for palaeoclimate reconstruction, especially for assessing local temperature and changes in climate shown by $\delta^{18}O$ records serve as a base to define and date the stadials and interstadials (Ruddiman, 2013). The isotopic composition of ice is influenced by moisture source and transport paths. Oxygen may originate from different locations, and the longer it travels, the more negative its isotopic ratio becomes as result of repeated condensation and evaporation of moisture. When heavier ^{18}O condenses, precipitation progressively removes it from the transported air mass. In result, the moisture reaching Greenland is depleted in ^{18}O, this happens during cold climate regime and shows in lower $\delta^{18}O$ value. Other factors determining the $\delta^{18}O$ values include changing a source site, source temperatures, and the seasonality of snowfall (Steffensen *et al.*, 2008). In Greenlandic ice cores, oxygen isotope values during interstadials are less depleted in ^{18}O compared to stadials. This shift can vary in $\delta^{18}O$ results by more than 5‰ as the climate changes (Ruddiman, 2013).

In addition, calcium ion concentration data highlights stadials and interstadials in ice cores. (Rasmussen *et al.*, 2014). [Ca^{2+}] is a common proxy of aerosol emitted to the atmosphere. Meteorological conditions shaped by long-term trends influence the concentration of dust in the atmosphere . Significant fluxes observed during stadials and interstadials reflect emission of dust from arid regions and/or changes in atmospheric circulation pattern (Kutuzov *et al.*, 2019). During cold and windier stadial events, atmospheric transport of aerosols increases, resulting in elevated concentration preserved in Greenland ice core records. In contrary interstadials are characterised with warmer and less windy conditions, hence the concentration in proxy records is lower (Rasmussen *et al.*, 2014).

2.3.4. Bermuda Rise, the North Atlantic Ocean records

In early 2000s, the gravity core OCE326-GGC5 was recovered from the Bermuda Rise located in the north-western subtropical Atlantic Ocean. The site is located at 33.42°N, 57.35°W (Fig. 3), at a depth of 4,550 m below the sea surface level. The Bermuda Rise is characterized by high-accumulation-rate; this allowed to assess 20,000 years of changes in ocean circulation (McManus *et al.*, 2004).

The chronology was established by expedition based on radiocarbon dating (^{14}C) from monospecific foraminifera samples collected from multiple depths throughout the sequence of 4.07 m long core. In addition to establishing sediment ages, the main objective was to assess the ^{231}Pa/^{230}Th ratio, which is directly connected to changes in the strength of meridional overturning circulation (McManus *et al.*, 2004).

The Atlantic meridional overturning circulation is a combination of North Atlantic Current and compensating south-flowing North Atlantic Deep Water (NADW). The Gulf Stream current flow transports warm, salty water by south-westerly prevailing winds. As it cools in the region of south of Greenland and in the Norwegian Sea, it becomes denser and sinks feeding south flowing, cold current (Lowe and Walker, 2014). This thermohaline circulation (THC) is widely believed to affect climate (Lowe and Walker, 2014; McManus *et al.*, 2004).
Production of ^{231}Protactinium and ^{230}Thorium (^{231}Pa/^{230}Th) takes place at a constant rate in seawater by uranium decay. Both isotopes are exposed to rapid removal by adsorption on settling particles from sea water and export to the sediments. As a result, the residence times in the water are relatively short; however, ^{231}Pa has a longer (±100-200 years) residence time and is relocated by NADW, compared to ^{230} Th (±20-40 years). Based on that difference in ratio, it is possible to establish the deep-water residence time and export based on accumulation rate of the ^{231}Pa/^{230}Th ratio based on ^{238}Uranium and ^{232}Thorium (McManus *et al.*, 2004).

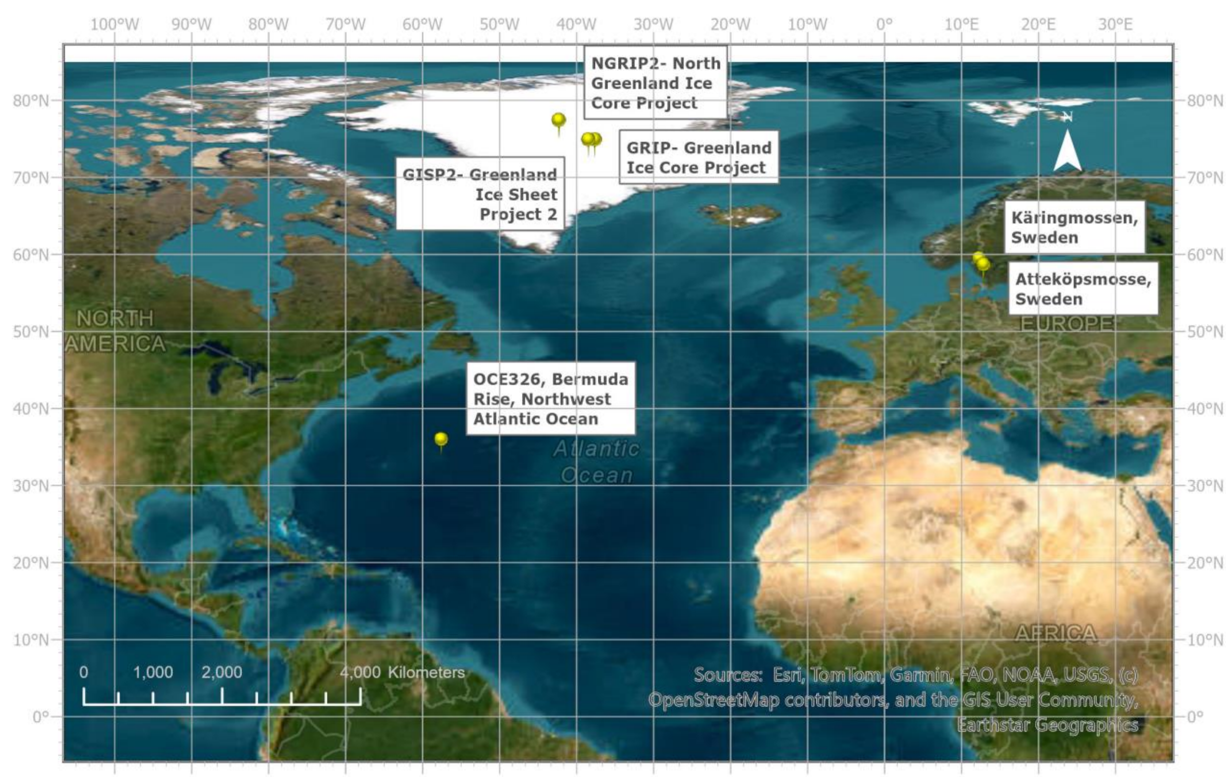

Figure 3. Location of archives used for this study.
The map illustrates the locations of multi-archive proxy used for this study. The OCE326 is marine sediments record from Bermuda Rise in North Atlantic Ocean; Atteköpsmosse and Käringmossen in Sweden are locations of peatlands archives, and GISP2, GRIP and NGRIP are ice core records in Greenland. Together, these locations provide a cross-regional framework for analyzing synchronized, environmental shifts within marine, terrestrial, and ice core archives.

Basemap: ArcGIS Pro; Coordinate System: WGS 84

3. Methods

Data were collected following a multi-proxy method. Pollen assemblages from Atteköpsmosse and Käringmossen, a July temperature reconstruction based on chironomid records for Atteköpsmosse, oxygen isotope ($\delta^{18}O$) and calcium ion [Ca^{2+}] records from NGRIP, GRIP and GISP 2 Greenland ice core and $^{231}Pa/^{230}Th$ ratio from North Atlantic Ocean marine records were compiled to reconstruct high-resolution climatic records following the changes in ocean-atmosphere interaction during 15.5-11.0 ka BP. All proxy records were plotted together and put on a common timescale to compare trends, timing and climatic responses.

The graphical analyses were performed in Microsoft Excel, and results were presented in PAleontological STatistics (PAST). Each diagram was adjusted to represent a studied time interval as closely as possible. Adjustments made during the analysis are described where relevant. Age is displayed in calibrated years before present (cal yr BP) and was plotted on the x- axis (abscissa), and each proxy result was presented on the y-axis (ordinate). This form was applied to all graphs presented in this study.

3.1. Pollen

3.1.1 Data

For Käringmossen, pollen samples were originally collected and counted by Palmgren (2023) from core KÄR01 (100-469 cm) and KÄR05 (0-100 cm). The total of 31 sediment samples were collected across the full depth range (0-469 cm).
For this study the interval of interest, defined as 15.5-11.0 ka BP is located between 300-469 cm corresponding to 10,995- 15,202 cal yr BP respectively. Based on the median age-depth reconstruction, the pollen sample closest to the depth of the upper boundary of this interval is located at depth of 297 cm which corresponds to 10,939 cal yr BP, while the deepest sample at 469 cm from 15,202 cal yr BP. Palmgren (2023) derived an age-depth model for the interval by linearly interpolated between 19 depth-age control points. Subsequently, pollen data for 6 taxa from 19 depths were used for this study based on Palmgren (2023) work.

For Atteköpsmosse, the dataset from Wohlfarth *et al.* (2018) was sourced from Bolin Centre Database

Following the stratigraphic alignment from core C-2011, the depth of interest to cover 15.5-11.0 ka cal yr BP in core C-1981 spans between 600-425 cm, corresponding to approximately 15,310- 11,450 cal yr BP. The available pollen dataset from Wohlfarth *et al.* (2018) covers depth between 597.5- 422.5 cm, and the sample depths were interpolated between sample points to match the age interval. A total of 30 pollen samples were analysed over this depth interval (Wohlfarth *et al*., 2018).

3.1.2. Investigated taxa

Atteköpsmosse and Käringmossen peatlands contained well-preserved pollen grains and spores' assemblages, which were counted and identified to the smallest taxonomic unit possible by Palmgren (2023) and Wohlfarth *et al.* (2018). The oryginal analyses, yielded 67 plant and algae taxa at Käringmossen, and 69 at Atteköpsmosse respectively. Here, for consistent comparison, original pollen counts of selected taxa were grouped into plant type categories. For this study, the main categories considered were Tree, Herbs, Shrubs & Dwarf Shrubs.
The individual taxa were as follows: trees *Betula* and *Pinus*; herbs- *Artemisia*, *Oxyria-type*/*Rumex acetosella* (Käringmossen/ Atteköpsmosse) and *Poaceae*/*Gramineae* (Käringmossen/ Atteköpsmosse); dwarf shrubs *Ericaceae*. To ensure consistency between sites, suggested nomenclature throughout the study is used: *Oxyria* for *Oxyria-type*/*Rumex acetosella*, and *Poaceae* for *Poaceae/Gramineae* consistent with Palmgren (2023). The pollen grains in Atteköpsmosse and Käringmossen were identified using different literature and keys, and therefore the pollen-type nomenclature differs between the sites.

After consultation with Palmgren Y. we decided to select *Betula* (birch), *Pinus* and *Artemisia* (sagebrush/mugwort). The main characteristics for birch, pine, and mugwort include adaptability in harsh environmental conditions, i.e. poor-nutrient or lack of soil, aridity or low temperature. Birch thrives in low competition areas and direct sunlight. Pine responds to environmental and temperature changes. These pioneer species adapt well in nutrient-poor and harsh environmental conditions. Importantly, birch and pine (assuming it was Scandinavian native *Pinus sylvestris* pollen found in records) temperature requirement is approximately 10/12°C. Their expansion observed within pollen records is evidence of postglacial warming and improvement in environmental conditions.

Important aspects of the Late Glacial period are the evolution of landscape openness and development of the soil. *Oxyria* (sorrel), *Poaceae* (grass), and *Ericaceae* (heath) were introduced to assess the dispersion rate in regards of the mentioned characteristics.
Sorrel is associated with cold and often sparsely vegetated environments. Its presence in sedimentary archives may indicate colder climatic conditions and open landscapes during the Late Glacial Period. Changes in abundance can provide useful information about postglacial vegetation development related to climate change and environment.
In the Late Glacial period, grasses are often associated with open habitats. Moreover, the taxon can be widely disperse and well preserved in sedimentary archives.
The heliophilous characteristic of heath, and high survival in nutrient-poor and acidic conditions is an

important indicator of the environment from late deglacial period. The pollen count, observed in both studied peatlands, makes it useful for proxy in palaeoenvironmental reconstruction.

Since both sites were lacustrine environments during the studied time interval, *Typha* (cattails) and *Nymphea* (water lilies) were considered as indicators of temperature and precipitation in the nearby environment. However, the decision to not include these aquatic taxa was motivated by the exclusivity to lacustrine conditions which can broadly vary and would not reflect the overall palaeoclimatic variability of both areas.

3.1.3. Pollen percentages and plotting

Percentage of pollen diagrams for six different taxa and plant type proportion for both Halland locations were presented in graphs for this study. To create an individual graph for *Betula*, *Pinus*, *Artemisia*, *Oxyria*, *Poaceae* and *Ericaceae* at each location, columns with depth and rows with taxa names were found in the pollen count section in work sheets provided by Palmgren (2023) for Käringmossen and by Wohlfarth *et al*. (2018) for Atteköpsmosse.
The calculation of the plant type ratio for both sites was made first. Then, the individual species of the Trees, Dwarf Shrubs & Shrubs, and Herbs were aggregated to determine the total count for each category.

To express these proportions as a percentage, the results are summarized for each depth, used in equation:

$$P_{planttype} = \left(\frac{n_{planttype}}{\Sigma n_{totalcategory}}\right) \times 100$$

Where
$P_{planttype}$- is the percentage of given plant type
$n_{planttype}$- is the pollen count of a plant type for that category
$\Sigma n_{totalcategory}$- is the total pollen sum of plant types of categories

Similarly, based on the assigned pollen type count, the following equation was used to calculate percentage of each taxon:

$$P_{taxon} = \left(\frac{n_{taxon}}{\Sigma n_{category}}\right) \times 100$$

Where:
P_{taxon}- is the percentage of specific taxon
n_{taxon}- is the taxa pollen count
$\Sigma n_{category}$- is the total count within the assigned plant category

The plant type ratio of Trees, Dwarf Shrubs & Shrubs, and Herbs for both locations, were presented with Stacked chart- stacked area method for both areas of study.

Percentage of individual taxa (*Betula*, *Pinus*, *Artemisia*, *Oxyria*, *Poaceae*, and *Ericaceae)* from both locations were plotted using XY line graph, to compare changes in pollen percentages with age. Finally, to compare both sites' age-depth models, the plotting function XY graph was applied where the data was shown in the continues line.

3.2. T-July Reconstruction Chironomids

July mean air temperatures were reconstructed for Atteköpsmosse using seven regional chironomid-based calibration models with dataset from unpublished internal dataset by Schenk (2026). The data used to present July Temperature reconstruction was based on the average over seven models, with temperature expressed in degrees Celcius (°C). 123 samples cover age between 15,425-11,120 median year BP, between depths 741-497 cm (Schenk, 2026. Unpublished).
The July Temperature Reconstruction for Atteköpsmosse was illustrated by plotting XY line graph.

3.3. $^{231}Pa/^{230}Th$ Ratio

For this study, the North Atlantic Core GGC5 $^{231}Pa/^{230}Th$ Meridional Circulation Data of McManus *et al.* (2004) was used, which provides $^{231}Pa/^{230}Th$ ratios, with associated error bars over the interval of 0.1-19.62 ka yr BP. Data were downloaded from National Center for Environmental Information (Centers and Centers, 2024).
The age value in the original dataset was presented in kilo years, these were converted to calibrated years before present, by multiplying each value by 1,000. This step was undertaken to unify data presented in the graph. The data were rendered into the program PAST and plotted by XY graph including error bars function where it was adjusted to present the interval 15,500-11,000 cal yr BP (McManus *et al.*, 2004).

3.4. Oxygen isotope $\delta^{18}O$ and calcium ion [Ca2+]

Combined dataset from the Greenland ice cores GRIP, GISP2 and NGRIP from Greenland, were synchronized by Seierstad *et al.* (2014) to produce a master chronology to 104 ka yr BP and provide 20-year and 50-year averaged $\delta^{18}O$ and [Ca^{2+}] data for each core (Seierstad *et al.*, 2014). The dataset consisting of 50-years means of oxygen isotope and calcium ion values on the GICC05modelext timescale was used to illustrate shifts in proxy values in this study.
Data Obtained from National Center for Environmental Information (Centers and Centers, 2025; Svensson *et al.*, 2008) was synchronized, and ages expressed in years before 2000 CE were changed to calibrated years before present, by subtracting 50 from each value. This conversion allowed finding an adequate depth for the study period for each ice core. The time interval of study can be located at depths in GRIP between 1577.52-1774.44 m; NGRIP2 between 1452.29- 1624.25 m; and GISP2 between 1633.83- 1817.56 m.
Variations of $\delta^{18}O$ in [‰] and concentration of [Ca^{2+}]in [ppm] from all three ice cores were illustrate with a help of XY graph method in PAST software for the selected age interval.

3.5. Sea level reconstruction

Differences in vegetation response between Atteköpsmosse and Käringmossen may be influenced by their proximity to the coastline and changing sea-level conditions during deglaciation, as well as by regional climate. To visualize the relationship between shoreline displacement and each site, data on the highest coastline in southwest Sweden were obtained and included in the reconstruction.
The data used for reconstruction of the highest coastline in Sweden was obtained from the SGU website (SGU, 2024). The GeoPackage was acquired from official website and processed using ArcGIS Pro software to visualize the spatial distribution of the highest postglacial coastline relative to the study sites in Sweden. The ArcGIS Pro project was referenced in the SWEREF99TM coordinate system to follow official geodetic referencing system used by Swedish Mapping, Cadastral and Land Registration Authority.
Both locations were marked on the map, using coordinates provided by Wolfhart *et al*. (2018) for Atteköpsmosse: 56°23'N, 12°51'E, and Palmgren (2023) for Käringmossen: 57°12'34.2"N, 12°16'52.7"E, which were translated to N 6343983 , E 335800 and N 6250819, E 367258 for suitable adjustment to SWEREF99TM. The relational database was created in Microsoft Excel software; locations name, Y, and X columns were made. Latitude values column Y and longitude value under column X, the data was later saved in .cvs format. A created table was imported to the ArcGIS Pro project and used to present exact locations of peatlands.
To ESRI-generated base map with satellite imagery, I added the highest coastline and location the Högsta kustlinjen (highest coastline) layer from the GeoPackage. The new layer with points of highest coastlines records and reconstruction of the shoreline created new map, which was integral map of changing coastline of southwest Sweden.

4. Results

This chapter presents the results of the multi-proxy analysis for southwest Sweden during the interval 15.5–11.0 ka BP. The results include reconstruction of shoreline displacement, comparison of chronological frameworks, and analysis of vegetation and climatic proxy records.

Figure 4 is comprised of 2 parts: Fig. 4a present assemblage of ratio from Atteköpsmosse and Käringmossen six individual taxa is compared with each other, and Fig. 4b shows pollen percentage from Atteköpsmosse and Käringmossen, T-July reconstruction assembly for Atteköpsmosse, AMOC $^{231}Pa/^{230}Th$ ratio, $\delta^{18}O$ value and $[Ca^{2+}]$ concentration from GRIP, GISP2 and NGRIP ice cores from Greenland. The results are presented on a common timescale.

Figure 4 presents all proxy data over the period 15.5 to 11.0 ka. The two pollen records begin shortly after 15.5 ka, corresponding to the end of the Oldest Dryas (GS-2.1a or Heinrich Stadial 1). Furthermore, the result emphasize Bølling period, which overlaps with onset of GI-1e. When comparing the pollen percentage records of *Artemisia* (Fig. 4.1d) and *Betula* (Fig. 4.1f), the general trend observed through the time interval resembles pollen abundance from Figure 4.2a. The dominance of herbs during the early Late Glacial period, later transition to tree dominant environment. Increased abundance of trees is especially seen in example of *Betula*, with significant spike in proportion starting at approximately 14,000 cal yr BP and remaining elevated until the end of records (approximately 11.5 ka BP). At the same time, *Atremisia* declined in abundance and remained stagnant until Holocene. This shift in plant percentage indicates a relatively prolonged and stable climate suitable for dispersion of the trees (Wohlfarth *et al.*, 2018).

The chironomid-inferred temperatures reconstruction ensembles for Atteköpsmosse (Figure 4.2b) (Schenk, 2026 unpublished) and oxygen isotope record from Greenland (Figure 4.2d), express a corresponding trend in relation to meridional circulation dynamic and overlaps with climatic periods discussed in this study (McManus *et al.*, 2004).

Over time, a slow development of the soils took place in southwest Sweden, which contributed to the distribution of vegetation i.e. *Poaceae* or *Eraceae* (Berglund *et al.*, 1994). *Ericaceae* (Fig 4.1a) was sparse at both locations until the end of Older Dryas, after which time the abundance increased at Käringmossen. However, it remained sparse in Atteköpsmosse throughout the duration of studied time. The influx of *Artemisia* and sorrel during Bølling can result from recently deglaciated terrain without developed soil, where lack of competition and their ability to tolerate a wide range of temperature served as an advantage for the taxa. However, both taxa percentage decreased in studied areas at the onset of warmer GI-1c3 events.

Presented in Figure 5 is the highest coastline reconstruction from spproximately 13.5 ka BP which was affected by i.e. glacial retreat, isostatic rebound, and catastrophic flooding. At Käringmossen, the reconstruction shows that the area was surrounded by the sea. Atteköpsmosse however, remained in close proximity to the highest coastline and wasn´t located on an island like Käringmossen. This could have influenced past prevailing microclimate. Käringmossen could experience more marine climate, whilst Atteköpsmosse-continental. This can reflect the vegetation variation and environmental development during 15.5-11.0 ka BP.

In Figure 6 records from Atteköpsmosse and Käringmossen do not entirely cover the studied time interval (15.5-11.0 ka BP). The temporal resolution of Atteköpsmosse indicates brief periods of enhanced sedimentation, e.g. Bølling; slower in YD. However, sedimentation rates with similar magnitude to each other at both locations. Further results for pollen and taxa abundance will therefore be justified.

A short period of the Oldest Dryas, at the end of GS-2.1a event or Heinrich Stadial 1, is overlapping the studied time proxy records. Pollen records at Atteköpsmosse end at approximately 15,310 cal yr BP and Käringmossen at about15,202 cal yr BP.

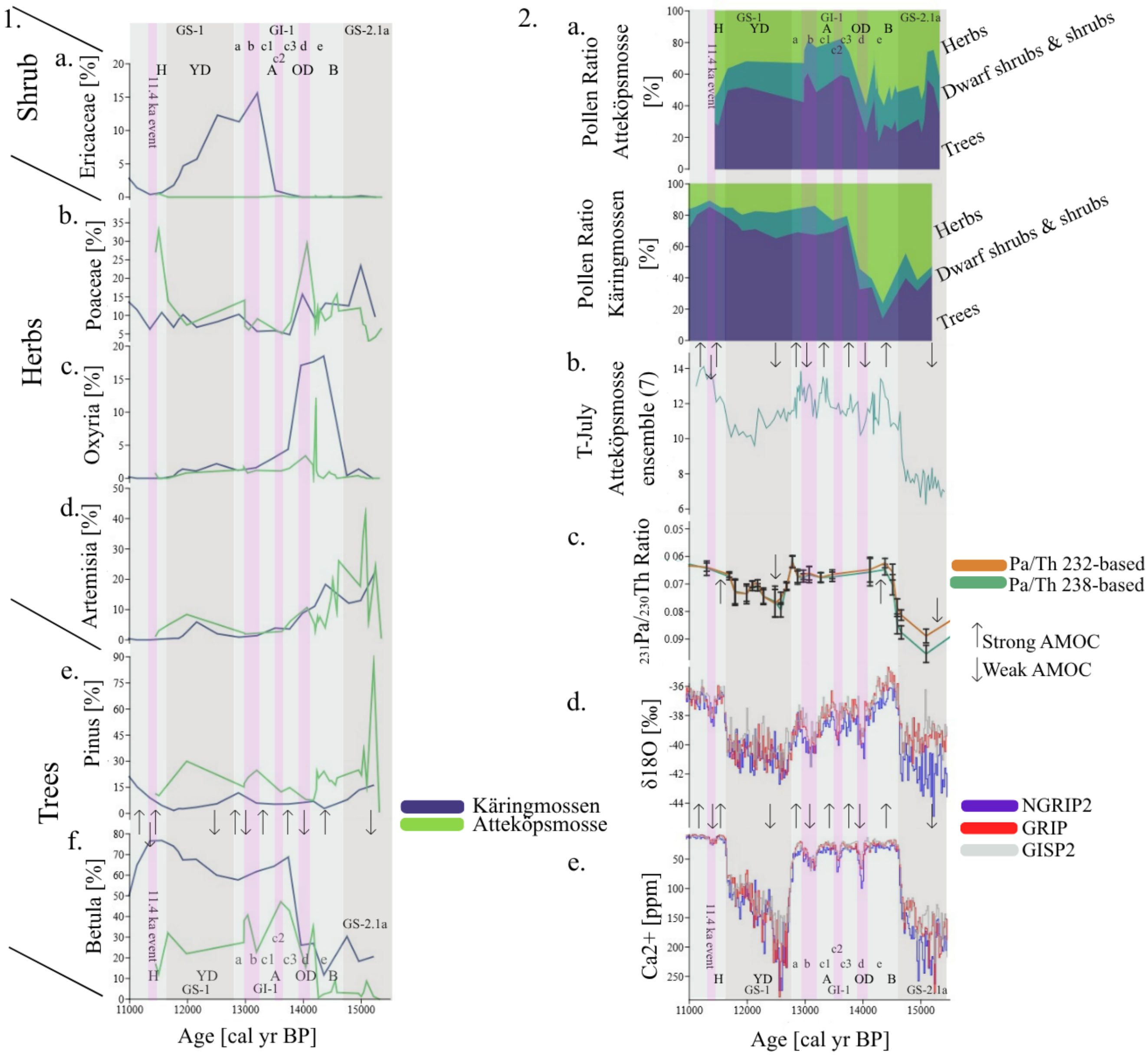

Figure 4. Assembly of multi-proxy data.

Figure 4.1 presents an assemblage of six taxa from Käringmossen (blue) and Atteköpsmosse (green). Figure 4.2 presents assemblage of a. pollen percentage at Atteköpsmosse and Käringmossen, b. T-July reconstruction ensemble for Atteköpsmosse, c. AMOC proxy, $^{231}Pa/^{230}Th$ ratio from Bermuda Rise, North Atlantic, arrows presents periods of weak and strong AMOC, d. oxygen isotope ($\delta^{18}O$) assemblage from NGRIP, GRIP, and GISP2 in Greenland, e. calcium ion [Ca^{2+}] assemblage from NGRIP, GRIP and GISP2 in Greenland. All proxy represents 15.5-11.0 ka BP interval. Abbreviations: H-Holocene, YD- Younger Dryas, A-Allerød, OD-Older Dryas, B-Bølling. Table 1 explains GI and GS positioning included in the time interval of study.

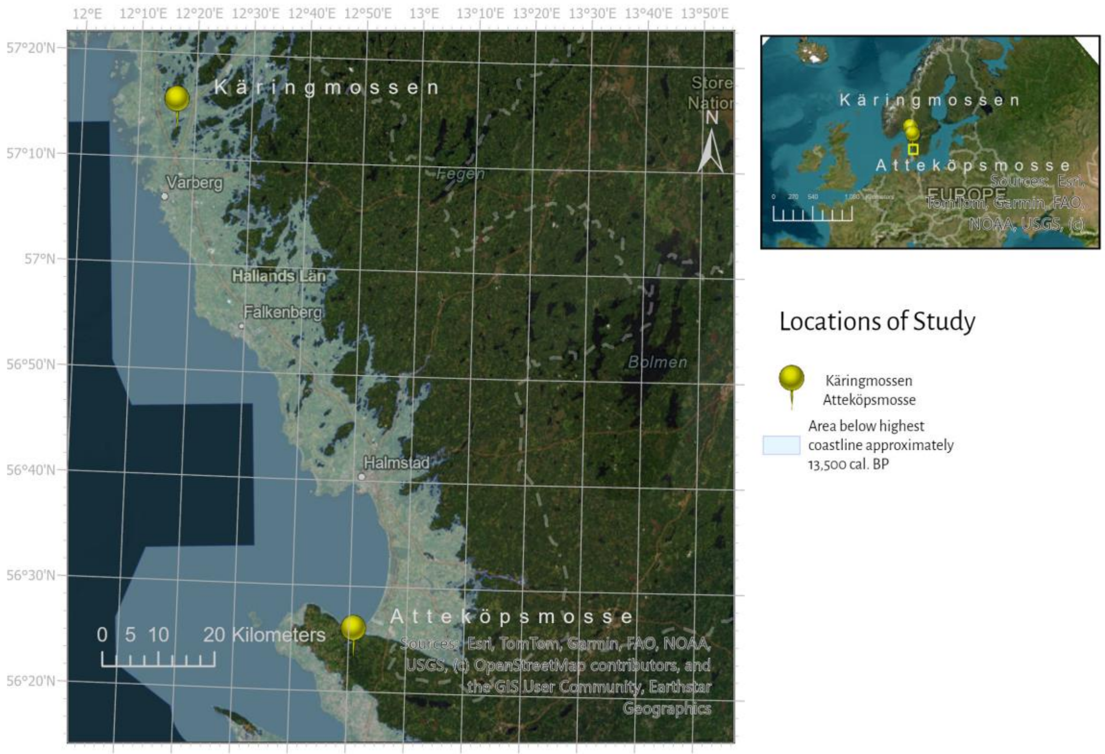

Figure 5. Highest Coastline Reconstruction Map.

The map illustrates the Shoreline Displacement Model during Late Glacial period (approximately 13,500 cal yr BP) shortly after deglaciation, included are Käringmossen and Atteköpsmosse, Halland, southwest Sweden.

Dataste: www.sgu.se; Basemap: ArcGIS Pro; Coordinate System: SWEREF99 TM

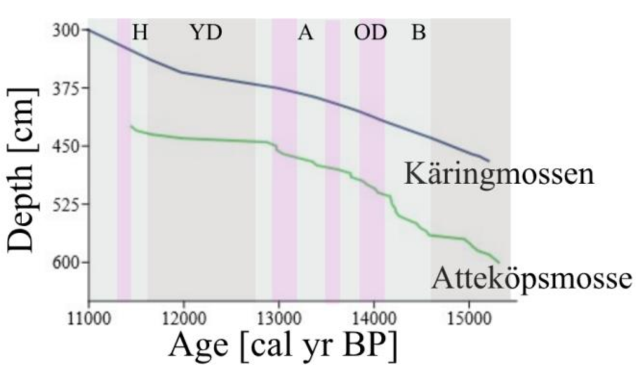

Figure 6. Age-depth model comparison.
Age-depth model for Käringmossen and Atteköpsmosse highlights the sedimentation rate during 15.5-11.0 ka cal yr BP. The highlighted time intervals are included based on the Greenland event stratigraphy, these are included for orientational purpose only and may not necessarily reflect local boundaries

4.1. The Oldest Dryas

The initial very high percentage of *Pinus* (Fig. 4.1e) in Atteköpsmosse distinctly decreased during the late GS-2.1a event, however this high proportion an be an effect of wind-transported pollen from afar to area of study, compromising the result of actual percentage. *Pocaeae* (Fig. 4.1b) and *Artemisia* (Fig. 4.1d) proportions are high on both sites.
July Temperature reconstructed for Atteköpsmosse oscillate between approximately 6°C and 8°C (Fig. 4.2b). The dominance in herbs (Non-arboreal) over trees (Arboreal) is observed in Käringmossen records. The pollen ratio of tree to herbs at Atteköpsmosse decreased toward the onset of the Bølling period (Fig. 4.2a).
The $^{231}Pa/^{230}Th$ ratio stays high at about 0.08 and even increases slightly to approximately 0.091 at around 15.1 cal yr BP (Fig. 4.2c). A high value suggests weak deepwater ventilation, hence very weak AMOC. Ice cores records from Greenland provide high resolution results from all three ice cores. The values of $\delta^{18}O$ are very low reaching approximately –44‰ (Fig. 4.2d), while [Ca^{2+}] concentration remain high reaching over 250 ppm (Fig. 4.2e) during that period reflecting a very dry conditions with high content of dust.

4.2. Bølling

The shift is documented by the percentage of *Betula* (Fig. 4.1f) in both locations. Abundance of herbs like *Oxyria* (Fig. 4.1c) and *Artemisia* (Fig. 4.1d) increased mainly in Käringmossen. The July Temperatures in Atteköpsmosse increased and oscillated between 10°C and 12°C degrees (Fig. 4.2b). The non-arboreal pollen dominated during the onset of Bølling in Atteköpsmosse and Käringmossen. Over time the result demonstrates an increase in arboreal pollen proportion at the end of the period (Fig. 4.2a).
The synchronization of the abrupt shift during the onset of Bølling is observed in Greenland and North Atlantic Ocean records as well as in temperatures of Atteköpsmosse. Pollen ratio, however, does not follow the same dynamic change. The vegetation response is somewhat stochastic in comparison to Greenland and North Atlantic records during Bølling, despite the temperature rise in Atteköpsmosse.
A steep increase of $\delta^{18}O$ values to -36‰ (Fig. 4.2d) in the Greenland ice cores is recorded, along with an abrupt decrease in [Ca^{2+}] concentration reduced to almost 0 ppm (Fig. 4.2e). $^{231}Pa/^{230}Th$ ratio which reached approximately 0.06 (Fig 4.2c). The results indicate increased strength of AMOC, providing a wetter and warmer climate.

4.3. Older Dryas

The percentages of *Poaceae*, *Oxyria* and *Artemisia* (Fig. 4.1.b, c, d) increased. At the same time, a brief but synchronous decline proportion of tree pollen abundance was observed at both Swedish locations at approximately 14,100 cal yr BP. The decline is emphasized by the percentage decrease of *Pinus* (Fig. 4.1e) and *Betula* (Fig. 4.1f). During the Older Dryas (OD), July temperature reached approximately

10°C at Atteköpsmosse, after an abrupt decrease at the onset of OD (Fig. 4.2b).
The $\delta^{18}O$ value decreased to about –40‰ (Fig 4.2d), while $[Ca^{2+}]$ concentration (Fig. 4.2e) increased which means colder and arid climate throughout duration of this brief period. Proxy records from Sweden and Greenland show synchronized response to the climate shift in their records however, there is no evident change in the AMOC recorded due to low resolution of the marine proxy record.

4.4. Allerød

An increasing trend in tree percentage through the Allerød, especially during GI-1c3 event at approximately 13,950 cal yr BP, is one of the main characteristics of this period observed at Atteköpsmosse and Käringmossen (Fig 4.2a). The abundance increase implies that trees were more established locally, in contrast to earlier fluctuation past arboreal proportion that were likely affected by wind-transported pollen from southern Europe. At the same time herbaceous representants, such as *Artemisia, (*Fig. 4.2d), display decreasing trends during this time interval. A significant increase in pollen percentage can be noticed in *Pinus* (Fig. 4.1e) proportion at both locations and *Ericaceae* (Fig. 4.1a) at Käringmossen.

The July temperature for Atteköpsmosse ranges between 11°C and nearly 14°C, with the most pronounced temperature drop during GI-1b event at the approximately 13,300 cal yr BP (Fig. 4.2b). Throughout the duration of interstadial (GI-1), the $^{231}Pa/^{230}Th$ ratio remains low and stable at about 0.065 with a brief decrease in ratio by the end of the event to approximately 0.061 (Fig. 4.2c). Throughout GI-1 there were two brief shifts in records during which $\delta^{18}O$ decreased at the onset of GI-1b and GI-c2 cooler events from an average of -38‰ to -40‰ (Fig. 4.2d), and at the same time $[Ca^{2+}]$ concentration increased in the Greenland records (Fig. 4.2e). This means a short and cold period during the overall warm trend during Allerød. The records show a synchronized proxy response during this fluctuation except for AMOC due to lower temporal resolution.

4.5. Younger Dryas

The overall cold climate of the Younger Dryas temporarily paused and somewhat lowered the previously rising proportion of arboreal and pollen for Atteköpsmosse and Käringmossen. Herbs proportion became briefly more dominant at both locations (Fig. 4.2a). The percentage of *Ericaceae, Poaceae* and *Betula* (Fig. 4.1.a, b, f) decreased only in Käringmossen, whereas *Artemisia* (Fig. 4.1d) increased in both Study Areas. Records of July Temperature reconstruction from Atteköpsmosse, shows fluctuation between approximately 9° and 12°C through the Younger Dryas (YD) period (Fig. 4.2b). The AMOC proxy ratio shifted abruptly to 0.08 and remained elevated throughout the cold interval (Fig. 4.2c). In the Greenland ice core records, $[Ca^{2+}]$ concentration increases to over ~250 ppm (Fig. 4.2e) simultaneously with the decreased $\delta^{18}O$ values to approximately –42‰ at the time of YD (Fig. 4.2d). All pollen proxy records show a synchronous response to the arid, cold conditions of this prolonged Greenland Stadial event.

4.6. Holocene

A short window of the early Holocene is included in the studied time interval. With a significant warming trend marking the onset of the Holocene, the 11.4 ka BP event highlights its presence with a brief decline in trees and shrubs pollen ratio at Käringmossen, including percentage of *Betula* (Fig. 4.1f) and *Poaceae* (Fig. 4.1b). Based on Rasmussen *et al.* (2014), a colder event took place at approximately 11.4 ka BP (Table 1), and its presence is marked in most proxy records included in this study. Pollen records at Atteköpsmosse begin at 11,450 cal yr BP, thus the time interval is not fully presented, and Pollen Ratio (Fig 4.2a) is decreasing right at the onset of Holocene.
The July temperature reconstruction from Atteköpsmosse oscillates between 12-14°C with an increasing trend. However, during the 11.4 ka BP event the temperature fluctuates at approximately 13°C (Fig 4.2b).
The $\delta^{18}O$ value and [Ca^{2+}] concentration during Holocene are comparable to a warmer interstadial of Late Glacial period. The Greenland ice core proxies show sensitivity to even short changes in environment including 11.4 ka BP event, where the overall isotopic enrichment oscillated at around -37‰ and depleted to about -38‰ during the event (Fig 4.2d).
The marine proxy record from Bermuda Rise presents a general shift into the warmer climate of the Holocene. $^{231}Pa/^{230}Th$ ratio decreases gradually from 0.065 and didn't record the 11.4 ka BP event (Fig. 4.2c).

5. Discussion

Comparison of pollen records to North Atlantic climate trends

The investigation primarily sought to interrogate whether, and to what extent, a perturbation in the Atlantic Overturning Meridional Circulation influenced the palaeoclimate of southwest Sweden during the 15.5-11.0 ka BP interval. The findings were derived from Greenland, North Atlantic Ocean and southwest Sweden records. The assembly of multiproxy results was formed, showing strength of AMOC, atmospheric temperature response, aridity, and response of vegetation to climate variability. The $^{231}Pa/^{230}Th$ ratio from a marine core OCE326 exhibit fluctuation in strength throughout the studied period of time. Lower ratio is a consequence of elevated AMOC strength, whereas higher ratio indicates a reduced strength of circulation. As a result, this fluctuation of northern oceanic heat transport regulates the delivery of heat from lower to higher latitudes (McManus *et al.*, 2004).
The proxy records from Atteköpsmosse and Käringmossen broadly correspond with major Late Glacial climatic shifts and support the interpretation that climatic conditions in southwest Sweden were influenced by AMOC variability during the studied interval. Primary results of comparing different proxies on the same time scale during Late Glacial period may be related to migration lag of plants, time lag in the establishment of vegetation or gradual soil development (Berglund *et al.*, 1994).

During the Late Glacial period, changes in northward oceanic heat transport may have contributed to changes across the North Atlantic region. During the Bølling-Allerød period an increased insolation and a shift in AMOC strength, contribute to warmer and wetter climate (Birks and Birks, 2014). Stronger and weaker AMOC phases can be associated with significant climate conditions shifts displayed in cryospheric dynamics of Greenland ice core records.

Pollen records from southwest Sweden, suggest a comprehensive increase in vegetation succession during GI-1 (approximately 14.65-12.95 ka BP), particularly pronounced in *Betula* and *Ericaceae* ratios. The transition from herb dominated to tree dominated environments, provides correlation to prevailing warmer and wetter climate during stronger AMOC phase which contributed to distribution of i.e. birch and pine which requires at least > 10°C to grow. The warming of the climate during Bølling- Allerød Interstadial allowed vegetation to expand after deglaciation (Birks and Birks, 2014; Rasmussen *et al.*, 2014). The same can be observed during the onset of Holocene (11.75 ka BP- present) (Birks and Birks, 2014).

An extensive warming during Bølling-Allerød period, led to significant ice sheet melting which released an abundance of fresh meltwater into the ocean, resulting in i.e. substantial sea level rise at the onset of B/A (Suzuki *et al.*, 2026). It also disrupted the Atlantic meridional overturning circulation, which over time weakened and contributed to climatic transition such as onset of the cooler Younger Dryas (Fig. 4.2c) (McManus *et al.*, 2004).

Decline in AMOC strength is reflected in the climate cooling expressed in Greenland and southwest Sweden proxy records. After the onset of GS-1 (approximately 12.95 ka BP), records show a halt and somewhat decrease in tree taxa (Fig. 4.1). This could have led to gradual disappearance from the area or local extinction forced by the deterioration of environmental conditions (Birks and Birks, 2014). The shift can correspond to a decrease in the local number of trees during YD which resulted in clearing the landscape. During that time, increased herb taxa such as *Artemisia*, *Oxyria* or *Poaceae* in Atteköpsmosse and Käringmossen records persisted during cooler period and also widely dispersed due to the recently open landscape. The end of the Oldest Dryas (15.55-14.65 ka BP) is also herb-dominated, indicating a sustained colder climate and poor soil conditions.

Comparison of trends at Atteköpsmosse and Käringmossen

The shift in pollen ratio is more abrupt in Atteköpsmosse conversely to gradual shift in Käringmossen (Fig. 4.2a) The climate on the island on which Käringmossen was located, could somewhat differ from the climate of Atteköpsmosse located near the coastline. Depending on the density, the heat capacity of water acts like thermal storage. Like in case of meridional overturning circulation, where the heat from warmer latitudes can be transported to distant locations, the proximity to the nearest water reservoir would consequently impact the micro-palaeoclimate. Surrounding water acts as a buffer between summer and winter temperatures, by lowering its amplitudes (Ruddiman, 2013). These may explain the vegetation response to marine and continental microclimate, shown as a graph with the local pollen ratio results for both sites (Fig. 4.2a). This helps to observe the stadial and interstadials from the perspective of two different microclimates. However, different resolutions of proxy data can also play a role in presenting the results. Appendix 1. and 2. provides insight into sites data resolution used in this study.

Uncertainties & limitation

Despite a successful presentation of a multiproxy perspective during Deglaciation, the results face some questions and limitations. The pollen proxy results are insufficient to determine to what extent the obtained archives solely correspond to AMOC-driven climate variability or whether and how they were influenced by the coastal positioning and associated microclimates. i.e. *Ericaceae* demonstrates an increase in pollen percentage at Käringmossen whereas Atteköpsmosse pollen remains on the same, low percentage (Fi. 4.1a). It is challenging to establish an AMOC signal-to-noise ratio for both locations.

Furthermore, considering that most selected taxa for this study are anemophilous (wind pollinated), the pollen could have been transported from afar and/or different locations. This could compromise the result to some extent and refute assumption about climatic characteristics assigned to the climate of studied time interval (Birks and Birks, 2014).

The importance of the palaeoclimate shift from 15.5-11.0 ka BP time interval translates to present time, where environmental changes enhanced by anthropological influence can take a similar abrupt path. Changes that occurred naturally in the past illustrate the sensitivity of climate to external non-anthropological forcing mechanisms. It is important to cautiously take comparisons of palaeo- and current climate, nonetheless it is important to understand and model trajectory of the changes based on the natural archives.

Although primary investigation of this study is relationship between AMOC and climate of southwest Sweden, it is important to mention that late-glacial climate and environment was also altered by multiple external mechanism including Milankovitch forcing, solar insolation, concentration of greenhouse gases in the atmosphere etc. Nevertheless, the influence of ocean circulation and AMOC impact was important on climate in Scandinavia, it is particularly during periods of abrupt climatic transition making it key focus of this study.

6. Conclusions

To answer questions about North Atlantic climate signals in southwest Sween during 15.5-11.0 ka BP, a multiproxy approach was applied. To evaluate the response of Atlantic overturning meridional circulation, an assembly of proxy records from southwest Sweden, Greenland and North Atlantic Ocean was created and analyzed.

The records from the last deglaciation, presented a close relationship between AMOC dynamics and climatic conditions in SW Sweden. The relationship is reflected in pollen assemblages from Atteköpsmosse and Käringmossen and a July temperatures reconstruction for Atteköpsmosse. Cold and arid climate conditions are associated with weaker AMOC stages and non-arboreal type of pollen, whilst warmer and wet climates are a result of a stronger AMOC phase and arboreal type of pollen. The synchronous yet somewhat delayed response of pollen increase is prominent during onset of Bølling-Allerød warm period, this correlate with warmer records from Greenland ice cores and stronger AMOC shown in North Atlantic records. The decrease, however is noted during the Younger Dryas climatic cooling, where AMOC proxy record show decline in strength leading to climatic response in Greenland and southwest Sweden records. The pollen assemblage emphasizes the impact of Atlantic meridional overturning circulation to Scandinavian region.

The research underscores the complexity of the North Atlantic climate signals which have impacted climate of southwestern Sweden. The multi-proxy palaeoclimate analysis demonstrated changes in strength of AMOC reflected in various records. This finding highlights the importance of ocean circulation dynamics of past climate variability and provides valuable context for climate prognosis and models for the local and regional scale.

The results demonstrated in this study connect the local responses to climatic shifts. The multiproxy approach demonstrated mutually supporting data, with a more detailed description of studied environments as opposed to a single-proxy approach.

Acknowledgment

I would like to express my sincere gratitude to Frederik Schenk, Ylva Palmgren and Sarah Greenwood for their invaluable support, guidance, and willingness to share their knowledge and resources throughout the process of writing this thesis. Their expertise and encouragement greatly contributed to both the scientific quality of this work and my personal development during this project. I am especially thankful for constructive feedback, and remarkable eagle eye during the final review of the thesis.
I would also like to thank my friends and family for their support. Finally, I would like to express my deepest gratitude to Tobias Hansson for the extraordinary support given to me while writing this thesis. Thank you for always believing in me and for helping me with the most important thing- giving me the time and possibility to fully dedicate myself to this work.

Reference list

Ågren, J., & Svensson, R. (2008). *Land uplift model and system definition used for the RH 2000 adjustment of the Baltic Levelling Ring*. In P. Knudsen (Ed.), *Proceedings of the 15th General Meeting of the Nordic Geodetic Commission*, Copenhagen, Denmark, 29 May–2 June 2006, pp. 84–92.

Andersen KK, Azuma N, Barnola JM, Bigler M, Biscaye P, Caillon N, Chappellaz J, Clausen HB, Dahl-Jensen D, Fischer H, Flückiger J, Fritzsche D, Fujii Y, Goto-Azuma K, Grønvold K, Gundestrup NS, Hansson M, Huber C, Hvidberg CS, Johnsen SJ, Jonsell U, Jouzel J, Kipfstuhl S, Landais A, Leuenberger M, Lorrain R, Masson-Delmotte V, Miller H, Motoyama H, Narita H, Popp T, Rasmussen SO, Raynaud D, Rothlisberger R, Ruth U, Samyn D, Schwander J, Shoji H, Siggard-Andersen ML, Steffensen JP, Stocker T, Sveinbjörnsdóttir AE, Svensson A, Takata M, Tison JL, Thorsteinsson T, Watanabe O, Wilhelms F, White JW; North Greenland Ice Core Project members (2004). High-resolution record of Northern Hemisphere climate extending into the last interglacial period. *Nature*, 431(7005), pp.147–151. doi:https://doi.org/10.1038/nature02805.

Beck, P., Caudullo, G., de Rigo, D. and Tinner, W., 2016. *Betula pendula, Betula pubescens and other birches in Europe: distribution, habitat, usage and threats*. In: J. San-Miguel-Ayanz, D. de Rigo, G. Caudullo, T. Houston Durrant and A.

Mauri, eds. *European Atlas of Forest Tree Species*. Luxembourg: Publications Office of the European Union, pp. e010226+. https://doi.org/10.2788/4251

Berglund, B.E., Björck, S., Lemdahl, G., Bergsten, H., Nordberg, K. and Kolstrup, E. (1994). Late Weichselian environmental change in southern Sweden and Denmark. *Journal of Quaternary Science*, 9(2), pp.127–132. doi:https://doi.org/10.1002/jqs.3390090206.

Berglund, M. (1995). Late Weichselian shore displacement in Halland, southwestern Sweden: relative sea-level changes and their glacio-isostatic implications. *Boreas*, 24(4), pp.324–344. doi:https://doi.org/10.1111/j.1502-3885.1995.tb00783.x.

Birks, H.H. and Birks, H.J.B. (2014). To what extent did changes in July temperature influence Lateglacial vegetation patterns in NW Europe? *Quaternary Science Reviews*, 106, pp.262–277. doi:https://doi.org/10.1016/j.quascirev.2014.06.024.

Björck, S., Walker, M.J.C., Cwynar, L.C., Johnsen, S., Knudsen, K.-L., Lowe, J.J. and Wohlfarth, B. (1998), An event stratigraphy for the Last Termination in the North Atlantic region based on the Greenland ice-core record: a proposal by the INTIMATE group. J. Quaternary Sci., 13: 283-292. https://doi.org/10.1002/(SICI)1099-1417(199807/08)13:4<283::AID-JQS386>3.0.CO;2-A

Blockley, S.P.E., Lane, C.S., Hardiman, M., Rasmussen, S.O., Seierstad, I.K., Steffensen, J.P., Svensson, A., Lotter, A.F., Turney, C.S.M. and Bronk Ramsey, C. (2012). Synchronisation of palaeoenvironmental records over the last 60,000 years, and an extended INTIMATE event stratigraphy to 48,000 b2k. *Quaternary Science Reviews*, 36, pp.2–10. doi:https://doi.org/10.1016/j.quascirev.2011.09.017.

Centers, N. and Centers, N. (2024). *NOAA/WDS Paleoclimatology - North Atlantic Core GGC5 231Pa/230Th Meridional Circulation Data*. [online] Noaa.gov. Available at: https://www.ncei.noaa.gov/access/metadata/landing-page/bin/iso?id=noaa-ocean-6406 [Accessed 5 March 2026].

Centers, N. and Centers, N. (2025). *NOAA/WDS Paleoclimatology - North GRIP - Greenland Ice Core Chronology 2005 (GICC05) 60,000 Year, 20 Year Resolution*. [online] Noaa.gov. Available at: https://www.ncei.noaa.gov/access/metadata/landing-page/bin/iso?id=noaa-icecore-6086&utm [Accessed 20 Mar. 2026].

Clark, P.U., Dyke, A.S., Shakun, J.D., Carlson, A.E., Clark, J., Wohlfarth, B., Mitrovica, J.X., Hostetler, S.W. and McCabe, A.M. (2009). The Last Glacial Maximum. *Science*, 325(5941), pp.710–714. doi:https://doi.org/10.1126/science.1172873.

Google Earth Pro 7.3.6 (2025), Map data: [56°23N,12°51E, Maxar Technologies, Imagery Date 19.05.2025] [Online]. Available at: https://www.google.com/earth/ (Accessed: 15 May 2026)

Grootes, P.M. and Stuiver, M. (1997). Oxygen 18/16 variability in Greenland snow and ice with 10−3- to 105-year time resolution. *Journal of Geophysical Research: Oceans*, 102(C12), pp.26455–26470. doi:https://doi.org/10.1029/97jc00880.

Haeften, S.V., Campbell, B.C., Milic, A., Addison-Smith, E., Kouba, J.A., Huete, A., Beggs, P.J. and Davies, J.M. (2023). Environmental DNA analysis of airborne poaceae (grass) pollen reveals taxonomic diversity across seasons and climate zones. *Environmental Research*, 247, pp.117983–117983. doi:https://doi.org/10.1016/j.envres.2023.117983.

Houssard, C. and Escarré, J. (1991). The effects of seed weight on growth and competitive ability of Rumex acetosella from two successional old-fields. *Oecologia*, 86(2), pp.236–242. doi:https://doi.org/10.1007/bf00317536.

Houston Durrant, T., de Rigo, D. and Caudullo, G., 2016. *Pinus sylvestris in Europe: distribution, habitat, usage and threats*. In: J. San-Miguel-Ayanz, D. de Rigo, G. Caudullo, T. Houston Durrant and A. Mauri, eds. *European Atlas of Forest Tree Species*. Luxembourg: Publications Office of the European Union, pp. e016b94+. https://doi.org/10.2788/4251

Hughes, A.L.C., Gyllencreutz, R., Lohne, Ø.S., Mangerud, J. and Svendsen, J.I. (2015). The last Eurasian ice sheets – a chronological database and time-slice reconstruction, DATED-1. *Boreas*, 45(1), pp.1–45. doi:https://doi.org/10.1111/bor.12142.

K Kubitzki and Kadereit, J.W. (2004). *The Families and Genera of Vascular Plants*. Berlin: Springer.

Krugman, S. L. and Jenkinson, J. L., (1974). Pinus L. Pine In: Seeds of woody plants in the United States. In: C. S. Schopmeyer (ed.), Agriculture Handbook 450. Washington, DC: U.S. Department of Agriculture, pp. 598–638.

Li, L., Jiang, Z., Xiong, Y., Akogwu, C.O., Olutayo Mary Tolulope, Zhou, H., Sun, Y., Wang, H. and Zhang, H. (2024). Comparative Analyses of the Complete Mitogenomes of Two Oxyria Species (Polygonaceae) Provide Insights into Understanding the Mitogenome Evolution Within the Family. *International Journal of Molecular Sciences*, [online] 25(22), pp.11930–11930. doi:https://doi.org/10.3390/ijms252211930.

Lowe, J.J., Rasmussen, S.O., Björck, S., Hoek, W.Z., Steffensen, J.P., Walker, M.J.C. and Yu, Z.C. (2008). Synchronisation of palaeoenvironmental events in the North Atlantic region during the Last Termination: a revised protocol recommended by the INTIMATE group. *Quaternary Science Reviews*, 27(1-2), pp.6–17. doi:https://doi.org/10.1016/j.quascirev.2007.09.016.

Lowe, J.J. and Walker, M.J.C. (2014). *Reconstructing quaternary environments*. London: Routledge, Taylor & Francis Group.

Lu, L.-L., Jiao, B.-H., Qin, F., Xie, G., Lu, K.-Q., Li, J.-F., Sun, B., Li, M., Ferguson, D.K., Gao, T.-G., Yao, Y.-F. and Wang, Y.-F. (2022). Artemisia pollen dataset for exploring the potential ecological indicators in deep time. *Earth System Science Data*, [online] 14(9), pp.3961–3995. doi:https://doi.org/10.5194/essd-14-3961-2022.

McManus, J.F., Francois, R., Gherardi, J.-M. ., Keigwin, L.D. and Brown-Leger, S. (2004). Collapse and rapid resumption of Atlantic meridional circulation linked to deglacial climate changes. *Nature*, 428(6985), pp.834–837. doi:https://doi.org/10.1038/nature02494.

Mooney, H.A. and Billings, W.D. (1961). Comparative Physiological Ecology of Arctic and Alpine Populations of Oxyria digyna. *Ecological Monographs*, 31(1), pp.1–29. doi:https://doi.org/10.2307/1950744.

Nordqvist, B. (2003) "The last mammut hunters Den arkeologiska undersökningen vid Skatmossen under åren 2000 och 2003," I spåren efter de sista mammutjägarna– den arkeologiska undersökningen vid Skatmossen år 2000. 2003:1. Varberg: Varbergs fornminnesförening. Available at: http://www.varbergsfornminnesforening.se/arkiv/skrifter/2003_I_sparen_efter_de_sista_mammutjagarna.pdf.

Palmgren, Y. (2023). *Lateglacial and Holocene vegetational change in northern Halland, southwestern Sweden.* Master's Thesis, Stockholm University .

Påsse, T. (1990) Beskrivning till jordartskartan Varberg NO. Uppsala: Sveriges geologiska undersökning ; Liber distribution (Serie Ae, nr 102)

Påsse, T. (1990) Beskrivning till jordartskartan Varberg NO. Uppsala: Sveriges geologiska undersökning ; Liber distribution (Serie Ae, nr 102). Nordqvist, B. (2003) I spåren efter de sista mammutjägarna – den arkeologiska undersökningen vid Skatmossen år 2000. 2003:1. Varberg: Varbergs fornminnesförening. Available at: http://www.varbergsfornminnesforening.se/arkiv/skrifter/2003_I_sparen_efter_de_sista_mammutjagarna.pdf.

Påsse, T. and Daniels, J. (2015) Past shore-level and sea-level displacements. SGU Rapporter och meddelanden 137. Uppsala: Sveriges geologiska undersökning. Available at: https://resource.sgu.se/dokument/publikation/rm/rm137rapport/rm137-rapport.pdf.

Rasmussen, S.O., Bigler, M., Blockley, S.P., Blunier, T., Buchardt, S.L., Clausen, H.B., Cvijanovic, I., Dahl-Jensen, D., Johnsen, S.J., Fischer, H., Gkinis, V., Guillevic, M., Hoek, W.Z., Lowe, J.J., Pedro, J.B., Popp, T., Seierstad, I.K., Steffensen, J.P., Svensson, A.M. and Vallelonga, P. (2014). A stratigraphic framework for abrupt climatic changes during the Last Glacial period based on three synchronized Greenland ice-core records: refining and extending the INTIMATE event stratigraphy. *Quaternary Science Reviews*, 106, pp.14–28. doi:https://doi.org/10.1016/j.quascirev.2014.09.007.

Rasmussen, S.O., Dahl-Jensen, D., Fischer, H., Fuhrer, K., Hansen, S.B., Hansson, M., Hvidberg, C.S., Jonsell, U., Kipfstuhl, S., Ruth, U., Schwander, J., Siggaard-Andersen, M.-L., Sinnl, G., Steffensen, J.P., Svensson, A.M. and Vinther, B.M. (2023). Ice-core data used for the construction of the Greenland Ice-Core Chronology 2005 and 2021 (GICC05 and GICC21). *Earth System Science Data*, [online] 15(8), pp.3351–3364. doi:https://doi.org/10.5194/essd-15-3351-2023.

Rasmussen, S.O., Seierstad, I.K., Andersen, K.K., Bigler, M., Dahl-Jensen, D. and Johnsen, S.J. (2008). Synchronization of the NGRIP, GRIP, and GISP2 ice cores across MIS 2 and palaeoclimatic implications. *Quaternary Science Reviews*, 27(1-2), pp.18–28. doi:https://doi.org/10.1016/j.quascirev.2007.01.016.

Ruddiman, W.F. (2013). *Earth's Climate*. Macmillan Higher Education.

Rull, V. (2025). Insights on the indicator capacity of *Artemisia* pollen in pre-Holocene paleoecology. *Palynology*, 49(4). doi:https://doi.org/10.1080/01916122.2025.2499121.

Schenk, F., 2026. *July temperature reconstructions based on seven different regional Chironomid calibrations for Atteköpsmosse*. Unpublished data.

Seierstad, I.K., Abbott, P.M., Bigler, M., Blunier, T., Bourne, A.J., Brook, E., Buchardt, S.L., Buizert, C., Clausen, H.B., Cook, E., Dahl-Jensen, D., Davies, S.M., Guillevic, M., Johnsen, S.J., Pedersen, D.S., Popp, T.J., Rasmussen, S.O., Severinghaus, J.P., Svensson, A. and Vinther, B.M. (2014). Consistently dated records from the Greenland GRIP, GISP2 and NGRIP ice cores for the past 104 ka reveal regional millennial-scale δ18O gradients with possible Heinrich event imprint. *Quaternary Science Reviews*, 106(Quaternary Science Reviews 106 (2014) 29-46), pp.29–46. doi:https://doi.org/10.1016/j.quascirev.2014.10.032.

SGU (2024). *Strandlinjer*. [online] Www.sgu.se. Available at: https://www.sgu.se/produkter-och-tjanster/geologiska-data/allmant-geologi--geologiska-data/strandlinjer/?utm_source=chatgpt.com [Accessed 25 May 2026].

Sinnl, G., Winstrup, M., Erhardt, T., Cook, E., Jensen, C.M., Svensson, A., Vinther, B.M., Muscheler, R. and Rasmussen, S.O. (2022). A multi-ice-core, annual-layer-counted Greenland ice-core chronology for the last 3800 years: GICC21. *Climate of the Past*, [online] 18(5), pp.1125–1150. doi:https://doi.org/10.5194/cp-18-1125-2022.

Stanislav Kutuzov, Legrand, M., Preunkert, S., Ginot, P., Vladimir Mikhalenko, Shukurov, K.A., Полюхов, A.A. and Торопов, П.A. (2019). History of desert dust deposition recorded in the Elbrus ice core. *Atmospheric Chemistry and Physics*, 19(22). doi:https://doi.org/10.5194/acp-2019-411.

Steffensen, J.P., Andersen, K.K., Bigler, M., Clausen, H.B., Dahl-Jensen, D., Fischer, H., Goto-Azuma, K., Hansson, M., Johnsen, S.J., Jouzel, J., Masson-Delmotte, V., Popp, T., Rasmussen, S.O., Rothlisberger, R., Ruth, U., Stauffer, B., Siggaard-Andersen, M.-L. ., Sveinbjornsdottir, A.E., Svensson, A. and White, J.W.C. (2008). High-Resolution Greenland Ice Core Data Show Abrupt Climate Change Happens in Few Years. *Science*, [online] 321(5889), pp.680–684. doi:https://doi.org/10.1126/science.1157707.

Stroeven, A.P., Hättestrand, C., Kleman, J., Heyman, J., Fabel, D., Fredin, O., Goodfellow, B.W., Harbor, J.M., Jansen, J.D., Olsen, L., Caffee, M.W., Fink, D., Lundqvist, J., Rosqvist, G.C., Strömberg, B. and Jansson, K.N. (2016). Deglaciation of Fennoscandia. *Quaternary Science Reviews*, 147, pp.91–121. doi:https://doi.org/10.1016/j.quascirev.2015.09.016.

Suzuki, K., Yamamoto, M., Polyak, L., Irino, T., Yamanaka, T. and Nam, S.-I. (2026). Bølling-Allerød meltwater discharge from the Laurentide Ice Sheet: Arctic Ocean sedimentary evidence. *Global and Planetary Change*, 261, p.105406. doi:https://doi.org/10.1016/j.gloplacha.2026.105406.

Svensson, A.M.; Andersen, K.K.; Bigler, M.; Clausen, H.B.; Dahl-Jensen, D.; Davies, S.M.; Johnsen, S.J.; Muscheler, R.; Parrenin, F.; Rasmussen, S.O.; Röthlisberger, R.; Seierstad, I.K.; Steffensen, J.P.; Vinther, B.M. (2008-07-01): NOAA/WDS Paleoclimatology - North GRIP - Greenland Ice Core Chronology 2005 (GICC05) 60,000 Year, 20 Year Resolution. NGRIP,

GRIP and GISP2 δ18O and calcium concentration in 50 yrs means on the GICC05modelext timescale. NOAA National Centers for Environmental Information. https://doi.org/10.25921/pkqb-2w42. Accessed 20 March 2026

Wei, C., Jardine, P.E., Gosling, W.D. and Hoorn, C. (2023). Is Poaceae pollen size a useful proxy in palaeoecological studies? New insights from a Poaceae pollen morphological study in the Amazon. *Review of Palaeobotany and Palynology*, 308, p.104790. doi:https://doi.org/10.1016/j.revpalbo.2022.104790.

Wohlfarth, B., Luoto, T.P., Muschitiello, F., Väliranta, M., Björck, S., Davies, S.M., Kylander, M., Ljung, K., Reimer, P.J. and Smittenberg, R.H. (2018). Climate and environment in southwest Sweden 15.5–11.3 cal. ka BP. *Boreas*, 47(3), pp.687–710. doi:https://doi.org/10.1111/bor.12310.

Wohlfarth, B. (2018). Lateglacial and early Holocene multi-proxy data set for the ancient lake at Attekӧpsmosse, southern Sweden (Version 1). Bolin Centre Database. https://doi.org/10.17043/wohlfarth-2018-attekopsmosse-1 (accessed 02 February 2026).

Wright, C.W. (2019). *Artemisia*. Boca Raton: Crc Press.

Www.sgu.se. (2024). Shorelines. [online] Available at: https://www.sgu.se/produkter-och-tjanster/geologiska-data/allmant-geologi--geologiska-data/strandlinjer/ [Accessed 7 May 2026].

Appendix

Appendix 1

Table 1. Results of Trees, Dwarf Shrubs & Shrubs, and Herbs Ratio for Käringmossen, Halland, Sweden.

Age (cal yr BP)	Trees (%)	Dwarf shrubs & shrubs (%)	Herbs (%)
10,991	71,74	12,42	15,83
11126	80,57	5,35	14,08
11349	85,63	4,02	10,34
11553	81,43	3,81	14,76
11756	76,38	8,66	14,96
11841	74,28	8,01	17,72
11917	70,41	10,24	19,35
12149	71,40	11,44	17,16
12503	65,51	16,38	18,11
12874	69,43	15,10	15,47
13184	67,62	18,66	13,72
13491	69,74	7,24	23,03
13741	74,20	5,60	20,20
13960	32,99	13,03	53,97
14172	34,33	5,25	60,41
14355	14,49	10,06	75,45
14753	40,26	16,02	43,72
14958	32,11	6,91	60,98
15202	41,96	5,36	52,68

Appendix 2

Table 2. Results of Trees, Dwarf Shrubs & Shrubs, and Herbs Ratio for Atteköpsmosse, Halland Sweden.
C-1981 age based on core-to-core stratigraphic alignment based on C-2011 core chronology.

Age (cal yr BP)	Trees (%)	Dwarf shrubs & shrubs (%)	Herbs (%)
11450	29,26	17,25	53,49
11500	27,94	21,48	50,58
11660	50,00	13,87	36,13
11980	52,20	16,20	31,60
12970	42,60	24,66	32,74
12975	56,77	18,55	24,68
13040	61,32	20,36	18,32
13190	48,98	28,25	22,76
13610	59,75	22,88	17,37
13760	57,86	16,16	25,98
14040	23,89	17,61	58,50
14170	43,12	22,87	34,01
14180	52,83	24,26	22,90
14220	24,82	26,44	48,74
14230	41,32	22,20	36,48
14260	18,11	29,87	52,02
14350	28,50	12,38	59,11
14450	26,38	27,34	46,28
14480	25,34	18,95	55,71
	32,75	25,55	41,70
14550	31,64	22,40	45,96
14580	23,85	25,05	51,10
14950	31,93	21,22	46,85
15000	24,14	20,72	55,13
15040	31,51	19,04	49,45
15092	57,40	16,92	25,68
	32,74	19,64	47,62
15210	51,78	23,95	24,27
	46,71	13,82	39,47
15310	35,70	24,11	40,19